

NAVAL POSTGRADUATE SCHOOL

Monterey, California



THESIS

**INVESTIGATION OF MINIMUM RESOLVABLE
TEMPERATURE DIFFERENCE FORMULATION FOR
POLARIZED THERMAL IMAGING RANGE PREDICTION**

by

Edson F. C. Guimarães

September, 1999

Thesis Advisor:
Thesis Co-Advisor:

Alfred W. Cooper
Ronald J. Pieper

Approved for public release; distribution is unlimited.

REPORT DOCUMENTATION PAGE

Form Approved
OMB No. 0704-0188

Public reporting burden for this collection of information is estimated to average 1 hour per response, including the time for reviewing instruction, searching existing data sources, gathering and maintaining the data needed, and completing and reviewing the collection of information. Send comments regarding this burden estimate or any other aspect of this collection of information, including suggestions for reducing this burden, to Washington Headquarters Services, Directorate for Information Operations and Reports, 1215 Jefferson Davis Highway, Suite 1204, Arlington, VA 22202-4302, and to the Office of Management and Budget, Paperwork Reduction Project (0704-0188) Washington DC 20503.

1. AGENCY USE ONLY (Leave blank)	2. REPORT DATE	3. REPORT TYPE AND DATES COVERED	
	September 1999	Master's Thesis	
4. TITLE AND SUBTITLE INVESTIGATION OF MINIMUM RESOLVABLE TEMPERATURE DIFFERENCE FORMULATION FOR POLARIZED THERMAL IMAGING RANGE PREDICTION.			5. FUNDING NUMBERS
6. AUTHOR(S) Guimarães, Edson F. C.			8. PERFORMING ORGANIZATION REPORT NUMBER
7. PERFORMING ORGANIZATION NAME(S) AND ADDRESS(ES) Naval Postgraduate School Monterey, CA 93943-5000			
9. SPONSORING / MONITORING AGENCY NAME(S) AND ADDRESS(ES)			10. SPONSORING / MONITORING AGENCY REPORT NUMBER
11. SUPPLEMENTARY NOTES The views expressed in this thesis are those of the author and do not reflect the official policy or position of the Department of Defense or the U.S. Government.			
12a. DISTRIBUTION / AVAILABILITY STATEMENT Approved for public release; distribution unlimited.			12b. DISTRIBUTION CODE
13. ABSTRACT (maximum 200 words) Previous measurements have demonstrated that a polarization filter can increase ship-background temperature contrast in the infrared, while decreasing the received radiance. Application of this technique to increasing range for detection or recognition of ship targets is being investigated through detection range modeling for a generic FLIR sensor. Laboratory measurements have been made of effective Minimum Resolvable Temperature Difference (MRTD) of a serial-scan 8-12 μ m sensor for polarized and unpolarized radiation. A variety of standard four-bar target boards of varied spatial frequency and controlled bar-background temperature difference were used to construct MRTD vs. spatial frequency. Results were compared with model predictions using known or measured component parameters for the AGA-780 imager, showing close agreement for observations made by a "trained observer." A modified form of MRTD was developed for a polarized target using a reformulation of the thermal derivative of Planck's law. Modeled and measured values agreed closely for the unpolarized case, and also for both vertically and horizontally polarized cases when the appropriate parameters of the polarization filters were included. Mathematical analysis and measurement agreed in displaying an increase in MRTD with polarization. Predictions of maximum detection and recognition ranges using estimates of polarized effective target-background temperature difference indicated probable range improvement for sea surface degree of polarization in excess of 20%.			
14. Subject Terms Thermal Imaging Systems, Minimum Resolved Temperature Difference, Polarization Filters.			15. NUMBER OF PAGES 149
16. PRICE CODE			
17. SECURITY CLASSIFICATION OF REPORT Unclassified	18. SECURITY CLASSIFICATION OF THIS PAGE Unclassified	19. SECURITY CLASSIFICATION OF ABSTRACT Unclassified	20. LIMITATION OF ABSTRACT UL

NSN 7540-01-280-5500

Standard Form 298 (Rev. 2-89)
Prescribed by ANSI Std. Z39-18298-102

Approved for public release; distribution is unlimited

**INVESTIGATION OF MINIMUM RESOLVABLE TEMPERATURE
DIFFERENCE FORMULATION FOR POLARIZED THERMAL IMAGING
RANGE PREDICTION**

Edson F. C. Guimarães
Captain, Brazilian Air Force
B.S., Brazilian Air Force Academy, 1990

Submitted in partial fulfillment of the
requirements for the degree of

MASTER OF SCIENCE IN SYSTEMS ENGINEERING

from the

NAVAL POSTGRADUATE SCHOOL
September 1999

Author: Edson Fernando da Costa
Edson Fernando da Costa Guimarães

Approved by: Alfred W. Cooper
Alfred W. Cooper, Thesis Advisor

Ron J. Pieper
Ron J. Pieper, Thesis Co-Advisor

Dan C. Boger
Dan C. Boger, Chairman
Information Warfare Academic Group

ABSTRACT

Previous measurements have demonstrated that a polarization filter can increase ship-background temperature contrast in the infrared, while decreasing the received radiance. Application of this technique to increasing range for detection or recognition of ship targets is being investigated through detection range modeling for a generic FLIR sensor. Laboratory measurements have been made of effective Minimum Resolvable Temperature Difference (MRTD) of a serial-scan 8-12 μm sensor for polarized and unpolarized radiation. A variety of standard four-bar target boards of varied spatial frequency and controlled bar-background temperature difference were used to construct MRTD vs. spatial frequency. Results were compared with model predictions using known or measured component parameters for the AGA-780 imager, showing close agreement for observations made by a "trained observer". A modified form of MRTD was developed for a polarized target using a reformulation of the thermal derivative of Planck's law. Modeled and measured values agreed closely for the unpolarized case, and also for both vertically and horizontally polarized cases when the appropriate parameters of the polarization filters were included. Mathematical analysis and measurement agreed in displaying an increase in MRTD with polarization. Predictions of maximum detection and recognition ranges using estimates of polarized effective target-background temperature difference indicated probable range improvement for sea surface degree of polarization in excess of 20%.

TABLE OF CONTENTS

I. INTRODUCTION	1
II. FUNDAMENTALS	5
A. ELECTROMAGNETIC SPECTRUM	5
B. LAWS OF THERMAL RADIATION	7
1. Planck's Law.....	8
2. Wien's Displacement Law.....	9
3. Stefan-Boltzmann Law.....	10
4. Total Power Law.....	11
5. Kirchoff's Law.....	11
C. ATMOSPHERIC PROPAGATION	11
D. POLARIZATION	13
III. MINIMUM RESOLVABLE TEMPERATURE DIFFERENCE	17
A. SIGNAL-TO-NOISE RATIO AND NOISE EQUIVALENT TEMPERATURE DIFFERENCE	18
B. MINIMUM RESOLVABLE TEMPERATURE DIFFERENCE (MRTD)	25
C. MRTD WITH THE POLARIZER	30
1. "Thermal Derivative"	31
2. Polarizer Transmissivity	32
3. Polarizer MTF	33
IV. LABORATORY EXPERIMENTS	35
A. AGA 780	35
B. CALIBRATION	35
C. MODULATION TRANSFER FUNCTION	38
1. Cutoff	39
2. MTF	40
D. AGA MRTD	43
1. Unpolarized Case	43
2. Polarized Case	45
V. ANALYSIS OF THE RESULTS	49
A. THE RESOLUTION PROCESS	49
B. A PROPOSED METHOD OF CALIBRATION	53
C. CALCULATED DATA VERSUS MEASURED DATA	58
D. RANGE CALCULATION	61
VI. CONCLUSION	75
APPENDIX A. MATLAB SOURCE CODES	79
APPENDIX B. LABORATORY SETUP	125

APPENDIX C. SUMMARY OF THE IMAGES	129
APPENDIX D. MEAN RADIANCE (8-12μm)	131
LIST OF REFERENCES	133
INITIAL DISTRIBUTION LIST	137

ACKNOWLEDGMENT

This research received financial support of SPAWAR Systems Center (NRaD) for the development of the polarized imaging techniques. Partial support was also provided by the Naval Postgraduate School Direct Funding for Research.

I wish to express my gratitude to those who contributed to the successful and timely completion of this project. First I would like to thank Mr. Robert Sanders for his contribution in the Electro-Optics Laboratory during the data acquisition process. I also would like to thank Professor Ronald Pieper for actively participating during all the phases of this work, and for proofreading it.

My deepest gratitude goes to Professor Alfred Cooper, whose guidance was extremely important to the accomplishment of this mission. His patience, cooperation, and wisdom are the aspects of this thesis that will not appear in the footnotes, but will always be the soul of this work.

Finally, I would like to thank my parents, my wife Ligia, and my son Gustavo for their support and understanding during the development of this work.

X

I. INTRODUCTION

With the development of an increasingly sophisticated battlefield, military systems have become more dependent on high technology than ever. Among other essential systems necessary to achieve advantage against the opponent, thermal imaging systems have been demonstrated to be important in numerous applications. Detection, recognition, and identification from ground based, aerial, or space platforms are among missions performed with the use of electro-optic and infrared systems. Thermal Imaging Systems rely upon a type of signature found everywhere in nature: thermal radiation.

Thermal radiation exists in any body at temperatures greater than the absolute zero (0°K), which implies that, not only the target, but also the background and even the atmosphere will contribute to the overall radiation reaching the sensor. The limiting factor that will determine the possibility of performing some task is known as the target-to-background contrast (TBC).

Possible ways to improve the target-to-background contrast include enhancement of target signature or elimination of background radiation. The second one is of

the most interest for this thesis. Experiments have demonstrated that, under certain circumstances, the use of polarization filters can reduce sea background [Ref. 1]. The use of polarizers though, may interfere with the performance of the Thermal Imaging System.

The most used measure of performance for thermal imaging systems is the Minimum Resolvable Temperature Difference (MRTD), which is a laboratory parameter defined to determine the resolution of the overall system, including the operator. In order to estimate the efficiency in performing a given task under a given scenario, both the MRTD and the TBC are important. While the TBC is improved when the polarizer is used, the MRTD values are down graded. Trading off those two parameters will determine whether the probability of performing the task is improved.

The objective of this thesis is to investigate the effect of the use of polarization filters on the Minimum Resolvable Temperature Difference of thermal imaging systems. We will start Chapter II by presenting some fundamentals of the infrared technology. Chapter III will develop the mathematical formulation of the MRTD for both the polarized and unpolarized cases. The laboratory experiment and the analysis of the results will be

presented in Chapters IV and V respectively. Chapter VI will then summarize and conclude this work.

II. FUNDAMENTALS

The objective of this Chapter is to ensure that the reader understands the basic concepts of Infrared Radiation. It does not intend to be a complete reference on this subject, but only to highlight those aspects of Infrared Radiation addressed in this thesis.

A. ELECTROMAGNETIC SPECTRUM

The electromagnetic spectrum is divided in a "quasi-arbitrary" way. Its divisions, called bands, are distinguished from each other mostly by the methods used to produce and detect the radiation.

The infrared portion of the spectrum lies in the region between the visible and the microwave, and is subdivided in four regions. The first, from $0.7\mu\text{m}$ to $1.1\mu\text{m}$, is the near infrared (NIR) and is dominated by the reflected sun radiation. Low light level TVs, image intensifiers, and night vision devices operate in this region [Ref. 2]. The second region spans from $1.1\mu\text{m}$ to $2.5\mu\text{m}$ and is called the short wavelength infrared band (SWIR). The third region, the mid-wavelength infrared (MWIR), ranges from $2.5\mu\text{m}$ to $7.0\mu\text{m}$. It is common to consider this

region as spanning from $3\mu\text{m}$ to $5\mu\text{m}$, since atmospheric attenuation limits its useful range. The next region (LWIR) is the most important for this thesis, since it is where all the laboratory measurements were taken. It ranges from $7\mu\text{m}$ to $15\mu\text{m}$, but is also limited from $8\mu\text{m}$ to $12\mu\text{m}$ for practical use.

Figure 2.1 shows a pictorial representation of the electromagnetic spectrum, with special emphasis on the IR spectrum.

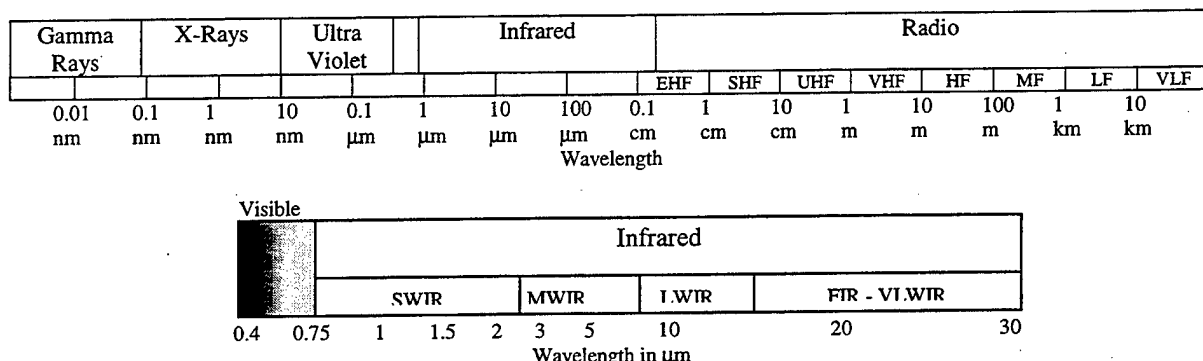


Figure 2.1 - The Electromagnetic Spectrum (After Ref. 5).

It is important to emphasize that, being part of the electromagnetic spectrum means that the infrared radiation obeys all the laws of electromagnetism, as stated by the Maxwell's Equations:

$$\Delta \times E = -\frac{\partial B}{\partial t} \quad (2.1)$$

$$\Delta \times H = J + \frac{\partial D}{\partial t} \quad (2.2)$$

$$\Delta \bullet D = \rho_v \quad (2.3)$$

$$\Delta \bullet B = 0 \quad (2.4)$$

where:

E = electric field intensity vector (V/m)

H = magnetic field intensity vector (A/m)

D = electric flux density vector (C/m²)

B = magnetic flux density vector (T)

J = electric current density (A/m²)

t = time (s)

ρ_v = volume charge density (C/m³)

B. LAWS OF THERMAL RADIATION

Before starting to enumerate the main laws of the thermal radiation, some definitions should be presented:

- Emissivity (ϵ): it is "the ratio of the radiant exitance or radiance of a given body to that of a blackbody." [Ref. 3]

- Blackbody: "it is an object which absorbs all radiation that impinges upon it at any wavelength." Blackbodies have, by definition, emissivity equal to unity ($\epsilon = 1$) [Ref. 4].
- Gray body: an object whose emissivity is high and fairly constant with wavelength. [Ref. 5]

Table 2.1 shows the most commonly used infrared quantities.

Quantity	Symbol	Units	Definition
Radiant Energy	U	Joules	
Radiant Power	P	Watts	$\partial U / \partial t$
Radiant Emittance	W	Watt/cm ²	$\partial P / \partial S$
Radiant Intensity	J	Watt/sr	$\partial P / \partial \Omega$
Radiance	N	Watt/cm ² sr	$\partial^2 P / (\partial S \partial \Omega)$

Table 2.1 - Radiometric Quantities (After Ref. 6).

1. Planck's Law

It describes the spectral distribution of the radiation from a blackbody, and is given by the following formula:

$$W_{\lambda,b} = \frac{2\pi hc^2}{\lambda^5 (e^{hc/\lambda kT} - 1)} \times 10^{-6} \quad (2.5)$$

where:

$W_{\lambda,b}$ = the blackbody spectral radiant emittance at wavelength λ (Watt/m² μm)

c = the velocity of light (3×10^8 m/s)

h = Planck's constant (6.6×10^{-34} Joule/s)

k = Boltzmann's constant (1.4×10^{-23} Joule/K)

T = absolute temperature of the blackbody (K)

λ = wavelength (m)

2. Wien's Displacement Law

By differentiating Planck's formula with respect to the wavelength (λ), and finding the maximum, we can establish the wavelength where the peak of radiation occurs for a given temperature. Wien's law is stated as:

$$\lambda_{\max} = \frac{2898}{T} \quad (2.6)$$

where:

λ_{\max} = wavelength where the peak of radiation occurs (μm).

This formulation can be graphically observed in Figure 2.2, where both Planck's and Wien's laws are plotted.

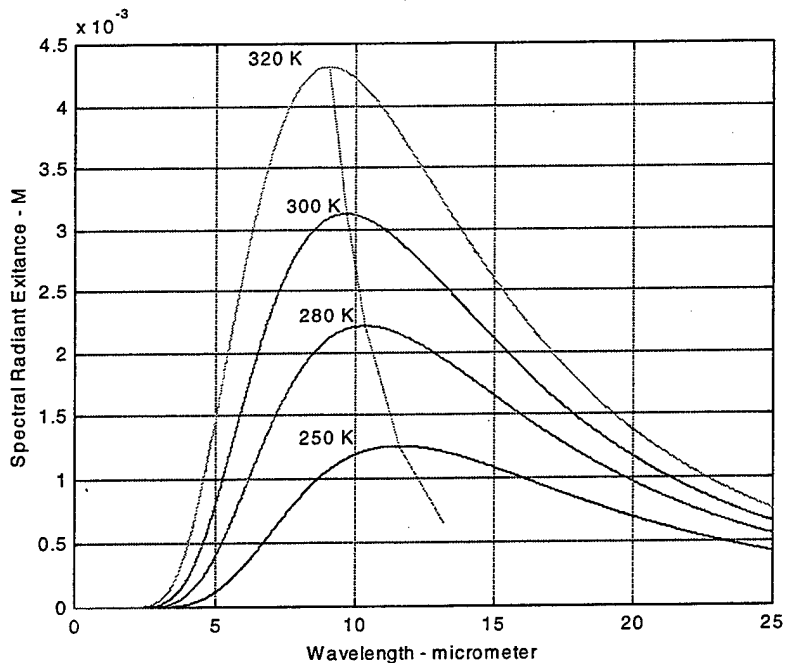


Figure 2.2 - Spectral Radiant Exitance of Blackbodies at Various Temperatures.

3. Stefan-Boltzmann Law

We can obtain the total radiant emittance of a blackbody by integrating Planck's law over the whole spectrum (from $\lambda=0$ to $\lambda=\infty$). It is known as the Stefan-Boltzmann Law, and is formulated as:

$$W_b = \sigma T^4 \quad (2.7)$$

where:

W_b = total radiant emittance of a blackbody

σ = the Stefan-Boltzmann constant (5.7×10^{-8} Watt/m²)

4. Total Power Law

"When radiation is incident upon a body, some of it is transmitted, some absorbed, and some is reflected. Thus the ratios of each of these to the incident power must add up to unity." [Ref. 3]

$$\alpha + \rho + \tau = 1 \quad (2.8)$$

where:

$$\alpha = \text{absorptivity} = P_{\text{absorbed}}/P_{\text{incident}}$$

$$\rho = \text{reflectivity} = P_{\text{reflected}}/P_{\text{incident}}$$

$$\tau = \text{transmissivity} = P_{\text{transmitted}}/P_{\text{incident}}$$

5. Kirchoff's Law

"Kirchoff's law of electromagnetic radiation states that a good absorber is also a good emitter of radiation by the equation:" [Ref. 6]

$$\alpha = \varepsilon \quad (2.9)$$

C. ATMOSPHERIC PROPAGATION

Four major phenomena occur when electromagnetic radiation propagates from a target to a sensor through the atmosphere: (1) its intensity is reduced, (2) atmospheric radiance is added to the target radiance, (3) non-scene radiance is scattered into the sensor, and (4) some scene

radiance is scattered away from the sensor. Those phenomena are illustrated in Figure 2.3.

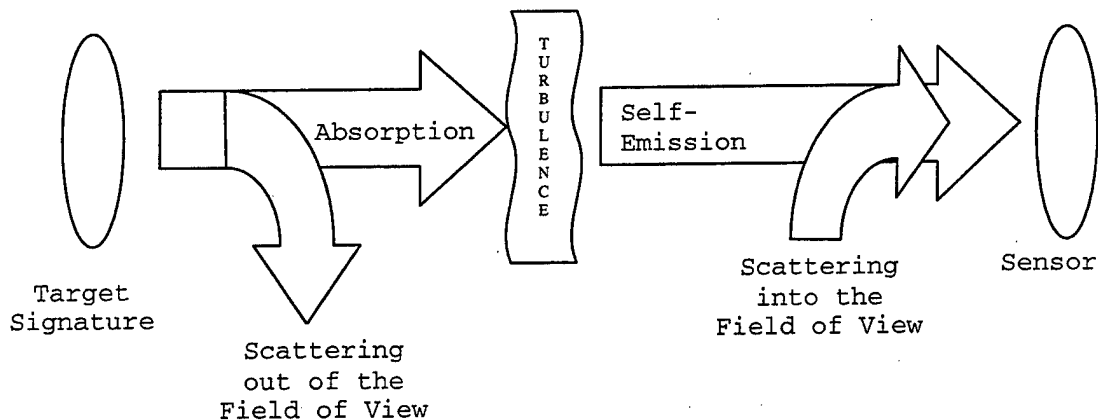


Figure 2.3 - Atmospheric Effects (After Ref. 2).

Two values are commonly used to define the atmosphere's behavior. The extinction coefficient ($\gamma(\lambda)$) represents the total reduction of radiation in the path from the source to the sensor, whereas transmittance ($\tau(\lambda)$) is defined as the ratio between the received radiance at the sensor to the emitted radiance from the source. It is not difficult to measure those values but it is very cumbersome to predict them, since the atmosphere is very dynamic and complex. Models have been proposed and some computer codes such as LOWTRAN, MODTRAN, HITRAN¹, and SEARAD² are used to obtain $\gamma(\lambda)$ or $\tau(\lambda)$.

¹ LOWTRAN, MODTRAN, and HITRAN - Low, Moderate, and High Resolution Transmission Code developed by the US Air Force (Geophysics Laboratory).

² SEARAD - Modification of MODTRAN developed by the US Navy (NRaD).

In this thesis, SEARAD will be used to predict atmospheric transmittance whenever needed. Figure 2.4 shows an example of transmittance values obtained from SEARAD. We can observe that wavelength severely affects the transmittance through the atmosphere, leaving us with two practical windows to work in: $3-5\mu\text{m}$ (MWIR) and $8-12\mu\text{m}$ (LWIR).

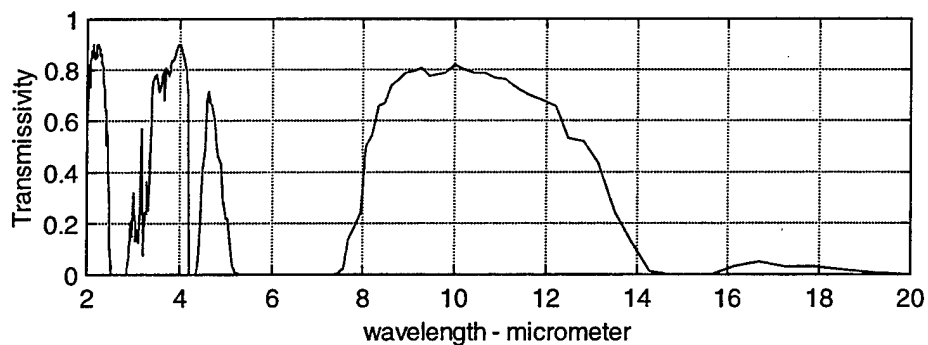


Figure 2.4 - Atmospheric Propagation (1 Km Horizontal Path Length, Midlatitude-Summer, Navy Maritime Aerosol, Airmass Characteristic = 3, Calculated Using Searad).

D. POLARIZATION

Electromagnetic waves (such as Infrared radiation) are composed of an electric and a magnetic field. Those fields are perpendicular to each other and perpendicular to the direction of propagation. Polarization of the wave is defined as the position of the electric vector as it progresses [Ref. 7].

The polarization of the wave may change in the boundary between two media. This phenomenon was studied by Fresnel, who proposed the following equation for nonmagnetic media:

$$r_{\text{perpendicular}} = -\frac{\sin(\theta_i - \theta_t)}{\sin(\theta_i + \theta_t)} \quad (2.10)$$

$$r_{\text{parallel}} = -\frac{\tan(\theta_i - \theta_t)}{\tan(\theta_i + \theta_t)} \quad (2.11)$$

$$t_{\text{perpendicular}} = \frac{2 \cdot \sin(\theta_t) \cdot \cos(\theta_i)}{\sin(\theta_i + \theta_t)} \quad (2.12)$$

$$t_{\text{parallel}} = \frac{2 \cdot \sin(\theta_t) \cdot \cos(\theta_i)}{\sin(\theta_i + \theta_t) \cdot \cos(\theta_i - \theta_t)} \quad (2.13)$$

where:

θ_i = incident angle.

θ_t = angle of transmission.

r = reflection coefficient.

t = transmission coefficient.

We must also define degree of polarization as:

$$POL = \frac{\langle N_v \rangle - \langle N_h \rangle}{\langle N_v \rangle + \langle N_h \rangle} \quad (2.14)$$

where:

$\langle N_v \rangle$ = mean apparent vertically polarized radiance.

$\langle N_h \rangle$ = mean apparent horizontally polarized radiance.

The Fresnel Equations demonstrate that, after reaching the boundary between two media, unpolarized incident radiation may be reflected with a certain degree of polarization, since the amount of parallel and perpendicular polarization components are reflected obeying different equations. At some angle (called the Brewster angle), we may have $r_{parallel}$ equal to zero and $r_{perpendicular}$ greater than zero. In this case, unpolarized radiation would reflect vertically polarized, which means a degree of polarization greater than zero.

III. MINIMUM RESOLVABLE TEMPERATURE DIFFERENCE

Minimum resolvable temperature difference (MRTD) is defined as the temperature difference between the background and a set of four standard bars (7:1 aspect ratio) required to make the bars just resolvable [Ref. 8]. It is the most used measure of performance for thermal imaging systems.

Before giving its complete mathematical formulation, it is necessary to highlight some important characteristics of the MRTD. First, it is a function of the entire system, including the observer. This implies the inclusion of some psychophysical aspects of human vision in the final formulation of the MRTD. Another important feature of the MRTD is that it is a function of the spatial frequency (Figure 3.1). It allows us to predict field performance of the thermal imaging system by establishing some criteria to convert object dimensions into spatial frequency.

There are several formulations used for the MRTD. In this work, we will use an approach similar to that proposed by Lloyd [Ref. 9]. Some concepts such as the signal-to-noise ratio (SNR) and the noise equivalent temperature difference (NETD) will be introduced prior to the MRTD.

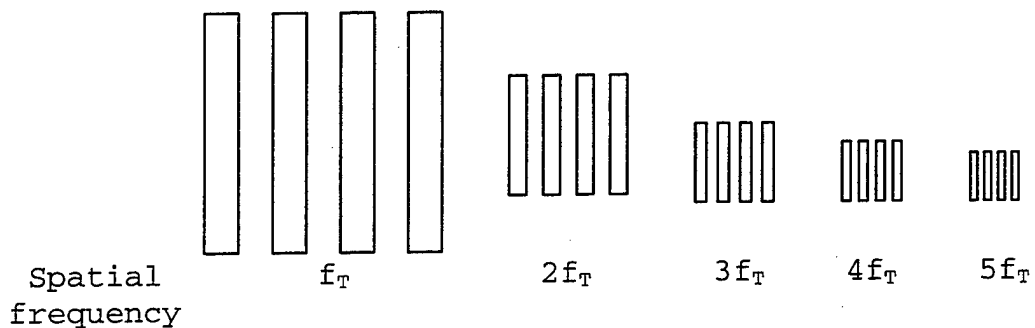


Figure 3.1 - MRTD Patterns of Differing Spatial Frequency.

A. SIGNAL-TO-NOISE RATIO AND NOISE EQUIVALENT TEMPERATURE DIFFERENCE

The first concept to be developed is the importance of the signal-to-noise ratio (SNR) in the thermal imaging process. The SNR gives a fundamental limit to the performance of a thermal imaging system. SNR is defined as the relationship between the signal and the noise level at the output of the system. It interferes with the observer's perception of the scene. It is usually used in an inverse form, as the noise equivalent temperature difference (NETD). NETD is the temperature difference between the signal and the background, which produces a SNR of one in the video signal.

$$NETD = \frac{\Delta T}{V_s/V_n} = \frac{\Delta T}{SNR} \quad (3.1)$$

where:

NETD = Noise Equivalent Temperature Difference ($^{\circ}$ K)

ΔT = Target-Background Temperature Difference ($^{\circ}$ K)

V_s = rms output signal voltage (V)

V_n = rms output noise voltage (V)

SNR = Signal-to-Noise Ratio

Noise equivalent temperature difference is obtained by considering a large target, surrounded by a large background (Figure 3.2), both with uniform temperature (T_t and T_b respectively).

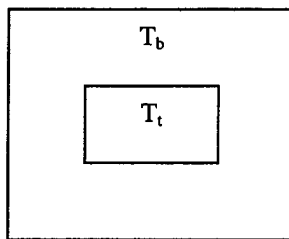


Figure 3.2 Target and Background Geometry.

Assuming a Lambertian surface, the spectral radiance of the surface is:

$$N_{\lambda} = \frac{W_{\lambda}}{\pi} \quad (3.2)$$

where:

N_{λ} = spectral radiance (watt/cm 2 μ m sr)

W_{λ} = spectral radiant exitance (watt/cm 2 μ m)

The instantaneous field of view subtended by the detector area ($a \times b$) is $\alpha \times \beta$, so that the detector receives power from the area $\alpha \times \beta \times R^2$ in the object plane. The spectral power at the aperture (Figure 3.3) is then given by the expression:

$$W_{\text{aperture}} = \frac{W_{\lambda} A_o \alpha \beta R^2}{\pi R^2} \quad (3.3a)$$

$$W_{\text{aperture}} = \frac{W_{\lambda} A_o \alpha \beta}{\pi} \quad (3.3b)$$

where:

W_{aperture} = spectral power at the aperture

A_o = aperture area (m^2)

a, b = detector dimensions (m)

α, β = detector instantaneous field of view (rad)

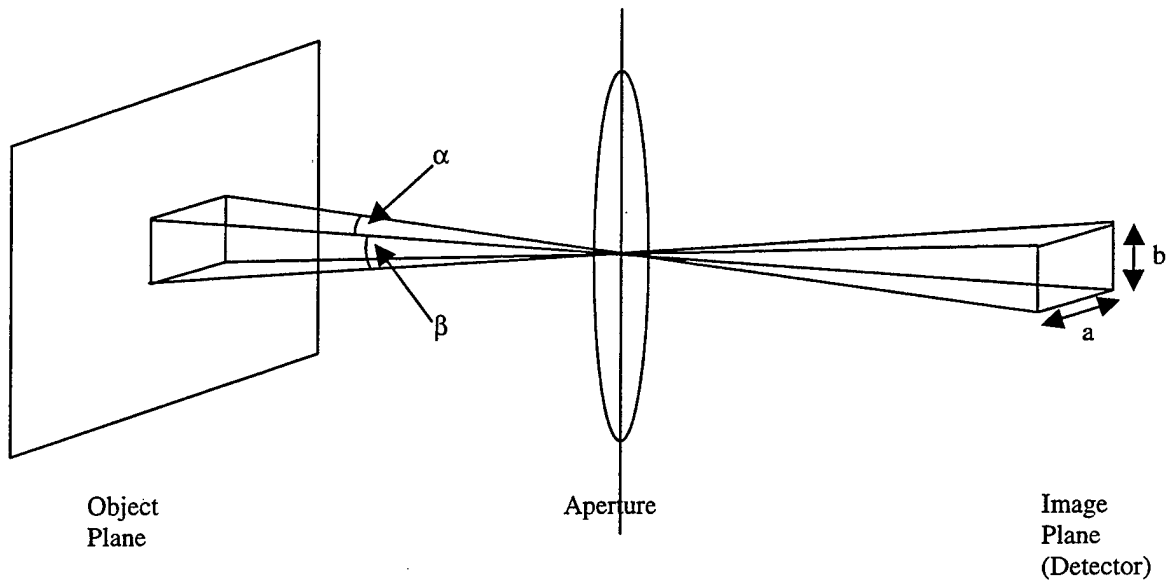


Figure 3.3 - Target/Detector Geometry.

Therefore, the power received by the detector is:

$$P_\lambda = \frac{W_\lambda}{\pi} \cdot A_o \cdot (\alpha\beta) \cdot \tau_o(\lambda) \quad (3.4)$$

where:

P_λ = power received by the detector (watt/ μm)

τ_o = transmissivity of the optical system

Hence, the differential power is:

$$\frac{\partial P_\lambda}{\partial T} = \frac{\alpha\beta}{\pi} \cdot A_o \cdot \tau_o \cdot \frac{\partial W_\lambda}{\partial T} \quad (3.5)$$

which gives a signal voltage of:

$$\frac{\partial V_s}{\partial T} = \frac{\alpha\beta}{\pi} \cdot A_o \cdot \tau_o \cdot \frac{\partial W_\lambda}{\partial T} \cdot R \quad (3.6)$$

where R (Responsivity in V/W) is given by:

$$R = \frac{V_n \cdot D^*(\lambda)}{\sqrt{a \cdot b \cdot \Delta f_n}} \quad (3.7)$$

and:

V_n = noise voltage in the bandwidth Δf_n (V)

D^* = Detectivity (cm Hz $^{1/2}$ W $^{-1}$)

Integrating Equation 3.4 over the wavelength, we have:

$$\frac{\Delta V_s}{V_n} = \Delta T \frac{\alpha \cdot \beta \cdot A_o}{\pi \sqrt{a \cdot b \cdot \Delta f_n}} \cdot \int_0^{\infty} \frac{\partial W_{\lambda}}{\partial T} \cdot D^*(\lambda) \cdot \tau_o(\lambda) \cdot d\lambda \quad (3.8)$$

Since we defined NETD as the ΔT for a SNR of one,

then:

$$NETD = \frac{\pi \sqrt{a \cdot b \cdot \Delta f_n}}{\alpha \cdot \beta \cdot A_o \cdot \int_0^{\infty} \frac{\partial W_{\lambda}}{\partial T} D^*(\lambda) \cdot \tau_o(\lambda) \cdot d\lambda} \quad (3.9)$$

For a system filtered to pass a selected band (λ_1 to λ_2), and assuming τ_o constant within that band,

$$\int_0^{\infty} \frac{\partial W_{\lambda}}{\partial T} D^*(\lambda) \cdot \tau_o(\lambda) \cdot d\lambda \equiv \tau_o \int_{\lambda_1}^{\lambda_2} \frac{\partial W_{\lambda}}{\partial T} D^*(\lambda) \cdot d\lambda \quad (3.10)$$

We define effective $\frac{\partial W}{\partial T}$ so that

$$\frac{\Delta W}{\Delta T} \cdot D^*(\lambda_p) = D^*(\lambda_p) \cdot \int_{\lambda_1}^{\lambda_2} \frac{\partial W}{\partial T} \cdot \frac{D^*(\lambda)}{D^*(\lambda_p)} d\lambda \quad (3.11)$$

where:

$D^*(\lambda_p)$ = detectivity at the peak wavelength (cm Hz $^{1/2}$ W $^{-1}$)

and:

$$NETD = \frac{\pi \cdot \sqrt{a \cdot b \cdot \Delta f_n}}{\alpha \cdot \beta \cdot A_o \cdot \tau_o \cdot D^*(\lambda_p) \cdot \frac{\Delta W}{\Delta T}} \quad (3.12)$$

Now, the Universal Radiation Curve can be used to evaluate $\frac{\Delta W}{\Delta T}$, and also,

$$\Delta f_n = \int_0^{\infty} S(f) \cdot H(f)^2 \cdot df \quad (3.13)$$

In Equation 3.13, Δf_n is the noise equivalent bandwidth of the reference filter, or equivalent external filter including the effect of all electronic MTF's, $S(f)$ is the noise spectrum (normalized), and $H(f)$ is the Modulation Transfer Function of the reference filter. This is related to the sensor dwell time τ_d .

$$H(f) = \left[1 + \left(\frac{f}{f_{3dB}} \right)^2 \right]^{-\frac{1}{2}}, \quad (3.14)$$

with

$$f_{3dB} \equiv \frac{1}{2 \cdot \tau_d}. \quad (3.15)$$

The filter is then suitably limited for the scanning rate, where twice the dwell time is equivalent to one period. Assuming the system has n detectors,

$$\tau_d = \frac{n \cdot \eta_{sc} \cdot \alpha \cdot \beta}{FOV_x \cdot FOV_y \cdot Fr} \quad (3.16)$$

where:

n = number of detectors

η_{sc} = scan efficiency

FOV_x and FOV_y = overall field of view (mrad)

Fr = frame rate (Hz)

We can finally write a formula for NETD that is convenient for trade-off analysis:

$$NETD = \frac{20 \cdot \sqrt{\pi \cdot a \cdot b \cdot FOV_x \cdot FOV_y \cdot Fr}}{\sqrt{n \cdot \eta_{sc} \cdot (\alpha \cdot \beta)^3 \cdot D_o^2 \cdot D^*(\lambda_p) \cdot \tau_o \cdot \frac{\Delta W}{\Delta T}}} \quad (3.17)$$

where:

$$D_o = \text{aperture diameter (m) is equal to } \sqrt{\frac{4 \cdot A_o}{\pi}}.$$

B. MINIMUM RESOLVABLE TEMPERATURE DIFFERENCE (MRTD)

As defined at the beginning of this Chapter, MRTD is a measure of the observer's ability to discern, at the output of a thermal imaging system (usually a gray scale display), a given spatial frequency. It includes some psychophysics of the human eye, such as eye/brain temporal integration and the effective narrow band-spatial filter of the eye.

The following assumptions are made:

- Spatial filtering in the eye, for a given target spatial frequency (f_T), is approximated by a matched filter with the following transfer function [Ref. 9, p.183]:

$$H_f = \text{sinc}\left(\frac{f}{2 \cdot f_T}\right) \quad (3.18)$$

- The amplitude of the fundamental frequency in the square wave is $4/\pi$ times the square wave amplitude,

$$R_{sw} = \frac{4}{\pi} [MTF_{system}] \quad (3.19)$$

where:

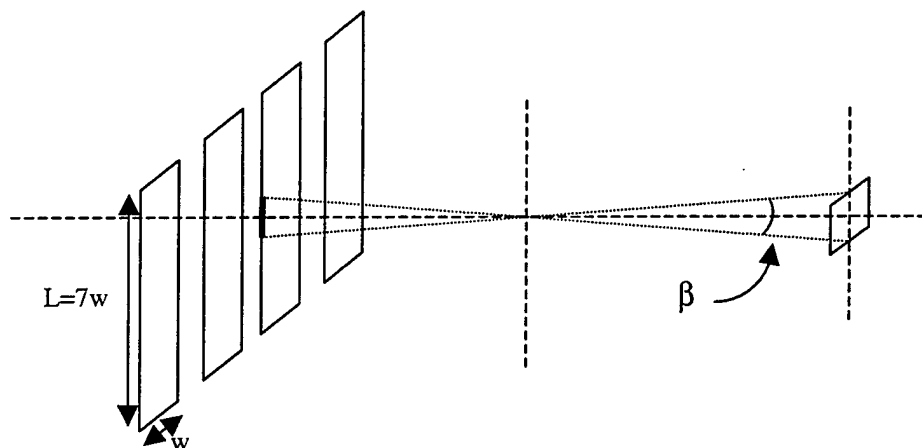
R_{sw} = square wave response of the system

MTF_{system} = modulation transfer function of the whole system

When the observer is introduced, some perception factors should be included [Ref. 9]:

- Eye signal averaging: the eye senses the mean signal of the image, which is $2/\pi$ for a half-cycle of the sine wave. This factor associated with the assumption stated in Equation 3.19 leads to a factor of $8/\pi^2$ when estimating the square wave by using a sine wave;
- eye integration time - Eye/brain integration time (T_e) is assumed to be approximately 0.2s, which improves the SNR by a factor of $(T_e Fr)^{1/2}$ [Ref. 9].
- the eye integrates the image along the bar (Figure 3.4). It gives an improvement factor in the signal-to-noise ratio of:

$$\left(\frac{L}{\beta}\right)^{1/2} = \left(\frac{7 \cdot w}{\beta}\right)^{1/2} = \left(\frac{7}{2 \cdot f_r \cdot \beta}\right)^{1/2} \quad (3.20)$$



Four Bar Pattern Target Aperture Detector

Figure 3.4 - Eye Integration along the Bar.

- eye spatial filtering: in order to account for the monitor and the observer, the new noise equivalent bandwidth becomes

$$\Delta f_n' = \int_0^{\infty} S(f) \cdot MTF_{monitor}^2 \cdot MTF_{amplifier}^2 \cdot \text{sinc}\left(\frac{f}{2f_T}\right) \cdot df \quad (3.21)$$

which corresponds to a SNR improvement of:

$$\rho^{1/2} = \left[\frac{\Delta f_n'}{\Delta f_n} \right]^{1/2} \quad (3.22)$$

Now, if we let the SNR_T be a minimum signal-to-noise ratio needed for detection of an individual bar, we can solve for ΔT as

$$\Delta T = \frac{NETD \cdot \rho^{1/2} \cdot \left(\frac{2 \cdot f_T \beta}{7} \right)^{1/2} \cdot SNR_T}{\left(\frac{8}{\pi^2} \right) \cdot MTF_{system} \cdot (T_e Fr)^{1/2}}. \quad (3.23)$$

The probability of detecting a single bar is a function of the SNR. Then, calculating the temperature difference corresponding to a desired SNR gives us the Minimum Resolvable Temperature Difference (MRTD)

$$MRTD(f) = \frac{NETD \cdot \rho^{1/2} \cdot (f_T \beta)^{1/2} \cdot SNR}{1.52 \cdot MTF_{system} \cdot (T_e Fr)^{1/2}}. \quad (3.24)$$

Finally, for white noise, ρ^2 can be approximated as

$$\rho^{1/2} = \left(\frac{2 \cdot f_T}{\tau_d \cdot \Delta f_n} \right)^{1/2} \quad (3.25)$$

and the final expression for the MRTD becomes

$$MRTD(f_T) = \frac{NETD \cdot SNR_T \cdot f_T (\alpha \beta)^{1/2}}{1.52 \cdot MTF_{system} \cdot (T_e Fr \tau_d \Delta f_n)^{1/2}}. \quad (3.26)$$

which is equivalent to Equation 5.58 in Lloyd [Ref. 9].

Various authors have proposed some alternative expressions for the MRTD. Shumaker et al [Ref. 8] give the following formula:

$$MRTD(f) = \frac{20 \cdot SNR_T \cdot (FOV_x \cdot FOV_y)^{1/2} f \cdot \rho_x^{1/2}}{\tau_o \cdot D \cdot D^* \cdot (\pi \cdot n \cdot \eta_{sc})^{1/2} \cdot (\alpha\beta)^{1/2} \cdot MTF_{system} \cdot (L \cdot T_e)^{1/2} \cdot \frac{\partial N}{\partial T}} \quad (3.27)$$

where:

SNR_T = perceived signal-to-noise ratio set according to the desired probability of performing the given task

f = spatial frequency (cycles/mrad)

D = aperture diameter (m)

D^* = detectivity ($\text{cm Hz}^{1/2} \text{ W}^{-1}$)

n = number of detectors

η_{sc} = scan efficiency

τ_o = transmission of the optics

α = in-scan detector angular subtense (mrad)

β = cross-scan detector angular subtense (mrad)

MTF_{system} = the system modulation transfer function

L = the length-to-width ratio for the bar chart (7)

T_e = eye integration time (0.2s)

$\frac{\partial N}{\partial T}$ = derivative of the Planck's Law ($\text{watt cm}^{-2} \text{ K}^{-1} \text{ sr}^{-1}$)

FOV_x = in-scan field of view (mrad)

FOV_y = cross-scan field of view (mrad)

ρ_x = noise filter factor

Equation 3.27 corresponds to substituting the expression for the NETD (Equation 3.17) in the formula for the MRTD (Equation 3.26).

In the next section, we will study the effects of the inclusion of a polarizer in the system.

C. MRTD WITH THE POLARIZER

In this section, we will propose a formulation for the MRTD for the case when a polarizer is added to the thermal imaging system. For simplicity, from now on, we will call it $MRTD_p$. In this study, all the parameters involved in the MRTD calculation were individually analyzed and their potential to affect the value of the $MRTD_p$ evaluated. The parameters considered to represent the greatest impact in this formulation are the polarizer transmissivity (τ_p), polarizer Modulation Transfer Function (MTF_p), and the partial derivative of Planck's Equation in relation to the temperature. They will be discussed in the rest of this section.

1. "Thermal Derivative"

The "thermal derivative" is the partial derivative of Planck's law with respect to temperature. It is a function of wavelength and the background temperature. Thermal imaging systems, in fact, do not measure temperature but radiance differences. Temperature difference (ΔT) is, however, a convenient concept and can be used when both the system spectral response and the background temperature are specified. [Ref. 2]

The addition of a polarizer in the system implies that a fraction of the total radiance will not reach the detector. For a perfectly unpolarized image (target and background), and assuming a perfect polarizer (efficiency equal to unity), this reduction would be fifty percent. However, in some situations, the concept of a perfectly unpolarized image is not met. For example, "Strong vertical polarization is observed in the sea surface emission near the Brewster angle in the $8-12\mu\text{m}$ (LWIR) band, whereas horizontal polarization due to reflection is usually dominant in the $3-5\mu\text{m}$ (MWIR) band." [Ref. 1] Exploring this effect would allow us to improve the overall contrast by

using a polarizer that filtered out the unwanted background radiation.

Since the "thermal derivative" is usually calculated and tabulated for a standard background temperature of 300 degrees Kelvin, our task is to estimate the value of background temperature that would reduce the total in-band radiance to one half of its previous value. In other words, we would need to solve the following equation

$$\int_{\lambda_1}^{\lambda_2} \frac{\partial N_\lambda(T_B)}{\partial T} d\lambda = k \cdot \int_{\lambda_1}^{\lambda_2} \frac{\partial N_\lambda(300)}{\partial T} d\lambda \quad (3.28)$$

where:

T_B = background temperature (K)

k = factor that represents the fraction of the total in-band radiance that reaches the detector, when the polarizer is used (0.5 for a perfect polarizer and a perfectly unpolarized image). When k is equal to 0.5, the equivalent value of T_B is 283K for the 3-5 μm band and 262K for the 8-12 μm band. [Ref. 8]

2. Polarizer Transmissivity

Another impact of the polarizer on the overall calculation is due to the fact that its transmissivity is different from unity. In fact, the transmissivity of the

polarizer used in this experiment (aluminum grid superimposed on KRS substrate manufactured by Graseby-Specac) is given by the manufacturer as being 0.85, for the electric vector aligned with the passage direction.

Considering that the impact of the loss in transmissivity would be equivalent to degrading the overall transmissivity of the optics, we would have

$$MRTD_p = \frac{MRTD}{k \cdot \tau_p} \quad (3.29)$$

where:

τ_p = polarizer transmissivity.

3. Polarizer MTF

Assuming the thermal imaging system is linear, its modulation transfer function is the result of the multiplication of the MTF of the individual subsystems (optics, stabilization element, detector, amplifiers, electronic filters, LEDs, visual optics and eye) [Ref. 2]. The addition of the polarizer to the system will include one more factor to the MTF

$$MTF_{\text{polarized system}} = MTF_{\text{polarizer}} \cdot MTF_{\text{unpolarized system}} \quad (3.30)$$

and it would affect the MRTD.

$$MRTD_p = \frac{MRTD}{MTF_{polarizer} \cdot \tau_p \cdot k} \quad (3.31)$$

Since the equipment necessary to measure the MTF of the polarizer was not available, we estimated it by measuring the MTF of the overall system with and without the polarizer. The results are shown in Chapter IV.

Since all values in the denominator of Equation 3.31 are less than one, we can expect the curve of the polarized MRTD to be shifted upward in relation to the unpolarized MRTD. This effect will be observed in the next chapter when we calculate the MRTD and the $MRTD_p$ for the AGA 780.

IV. LABORATORY EXPERIMENTS

A. AGA 780

The AGA Thermovision® 780 is a fourth generation dual-scanner thermal imaging system manufactured by AGA Infrared Systems AB, with headquarters in Danderyd, Sweden. In this experiment, only the LWIR band (8-12 μ m) was used and the system characteristics, when available, were obtained in the operating manual. Some parameters were not available and had to be estimated using typical values obtained in the literature.

B. CALIBRATION

As mentioned in Chapter I, the rate of emission of infrared radiation from a blackbody increases non-linearly with temperature. It is necessary to establish the correct relationship between actual object temperature and thermal imaging output. This is done by using calibration curves.

In the operation of the AGA 780, objects are characterized by temperature differences, but the analog output of the system is given in "isothermal units." Calibration curves are then used to transform isotherm

units into temperature for each configuration of the equipment (aperture and lenses). When digitization boards and digital data acquisition software are used, the fundamental output units will be "digital levels."

Digital Level (DL) is the scale used by the signal processing computer, and is dependent on the ADC boards and software used. For the PTRWin [Ref. 17] Data Acquisition and Processing System currently used with the AGA 780 imager at the Naval Postgraduate School this is based on a 12-bit output, ranging from 0 to 4095 ($2^{12} = 4096$ levels). Digital level values can be converted to Isothermal Units (IU). Isothermal units depend on two settings of the thermal imaging system, the thermal range, and the thermal level, and range from zero to 2000. By setting a thermal level, we establish the midscale level of thermal units allowed in the output. On the other hand, by setting the thermal range, we establish the variation from the midscale allowed in the output. For example, setting the thermal level to 100 and the thermal range to 20, we will have the output ranging from 90 to 110 IU. The thermal range is then divided into discrete steps, as allowed by the available digital levels. In the previous example, 20 IU is divided by 4095, to establish the correspondence that 1DL is

equivalent to 0.00488IU. The relationship between Digital Level and Isothermal Units is given by:

$$IU = \frac{DL \cdot Thermal_Range}{4095} + Thermal_Level - \frac{Thermal_Range}{2} \quad (4.1)$$

where:

IU = Isothermal Units

DL = Digital Level.

The conversion between Isothermal Units and Temperature is now obtained through calibration curves. In order to establish the calibration curves, laboratory measurements were performed following the steps given in the AGA 780 Operating Manual. Basically, a number of blackbody sources at different temperatures were measured with the system. The results were fed into a Matlab® program (Appendix A) that gives the least square fitting parameters for the following expression [Ref. 4]

$$IU = \frac{A}{\frac{B}{C \cdot e^T} - 1} \quad (4.2)$$

where:

IU = Isothermal Units

T = Absolute Temperature

A, B, C = Calibration constants that depend on actual aperture, filter scanner version, etc.

Table 4.1 shows the results obtained from these measurements, and the corresponding values of A, B, and C.

A Matlab® function was written to perform conversions between Digital Level and Temperature. This function, dl2temp.m, is shown in Appendix A.

Temperature (°C)	Filter Unpolarized	Temperature (°C)	Filter	
			Vertical Polarized	Horizontal Polarized
22	51	23	50	50
27	55	27	51	51
32	59	33	52	52
37	63	37	54	54
42	68	43	57	57
50	75	50	59	59
60	84	61	63	63
70	94	70	67	67
80	103	80	71	71
91	115	90	75	75
101	126	100	80	80
111	139	110	86	86
A	2.318E+3	A	5.679 E+3	5.679 E+3
B	1.218E+3	B	57.46	57.46
C	0.742	C	0.918	0.918

Table 4.1 - Output in Isothermal Units.

C. MODULATION TRANSFER FUNCTION

As observed in Equations 3.27 and 3.32, the Modulation Transfer Function (MTF) greatly impacts the final value of the MRTD. One important aspect to be pointed out is the fact that the MTF goes to zero at some value called the cutoff spatial frequency (Figure 4.4). It implies that the

MRTD curve will tend to asymptote at this cutoff frequency (Figure 4.5). In practice, most current thermal imaging systems have this cutoff at a frequency near the reciprocal of the detector angular subtense [Ref. 8]. The next section will show how the cutoff frequency for the AGA 780 was experimentally estimated.

1. Cutoff

During the preliminary measurements, it was observed that spatial frequencies greater than 0.6 cycles per milliradian could not be resolved by the system. In order to determine the exact value of the cutoff, the following approach was adopted. At 2 meters and using a standard four-bar pattern that had a bar width of 5mm, the output was recorded. Figure 4.1 shows the recorded profile of this output, using the "profile function" of the PTRWin® software [Ref. 17].

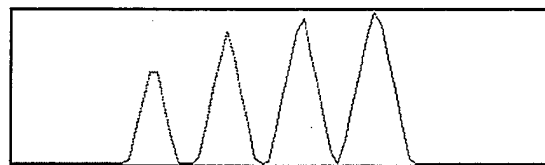


Figure 4.1 - Output of the System at 0.4cycles/mrad.

This corresponds to an angular resolution of $5\text{mm}/2\text{m} = 2.5\text{ mrad}$, which would give a cutoff of

0.4 cycles/mrad. Since the first peak still has a short flat top, we would infer that, in fact, the minimum angular resolution would be greater than 0.4 cycles/mrad. Then, at 2.75m and using a pattern with a spatial frequency of 0.55 cycles/mrad), we had the profile shown in Figure 4.2. This figure shows that a 5mm bar is represented by a single point, which indicates that the cutoff frequency of the system is, indeed, approximately 0.55 cycles/mrad.

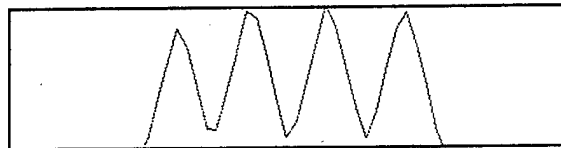


Figure 4.2 - Output of the System at 0.55 cycles/mrad.

2. MTF

The next step necessary to calculate the MRTD of the system was to determine the Modulation Transfer Function (MTF). MTF is a function of the spatial frequency that defines the ratio of the modulation in the observed image to that in the actual object, and is defined as in Equations 4.3 and 4.4 [Ref. 5]. Figure 4.3 shows the difference in modulation between the input and the output the system.

$$M(f) = \frac{V_{\max} - V_{\min}}{V_{\max} + V_{\min}}. \quad (4.3)$$

$$MTF = \frac{M_{out}(f)}{M_{in}(f)} \quad (4.4)$$

where:

$M(f)$ = Modulation

$M_{in}(f)$ = Modulation at the input

$M_{out}(f)$ = Modulation at the output

f = spatial frequency

V_{max} and V_{min} as shown in Figure 4.3.

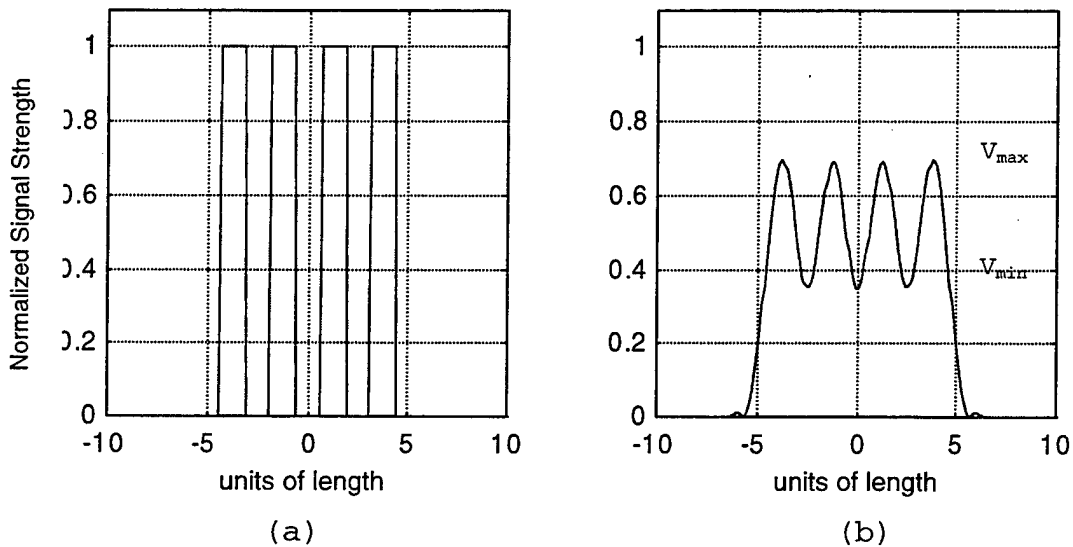


Figure 4.3 - Output Signal (b) Resultant of the Impact of the MTF on the Input Signal (a).

For the purpose of this thesis, the MTF of the AGA 780 was estimated by measuring and recording the output of the system at several selected spatial frequencies and

calculating the modulation of each one. The result is shown in Figure 4.4. The following step was to find a curve that best fitted the data. Using Matlab®, we generated a fitting algorithm (mtffit.m, Appendix A) that tried the several templates for the fitting curve:

- polynomial of degree 2 or 3;
- gaussian;
- typical lowpass filter; and
- "sinc" function.

Using the least square approach, the template that best fitted the data was

$$MTFfit(f) = \left(\frac{\sin\left(\frac{\pi \cdot f}{f_c}\right)}{\frac{\pi \cdot f}{f_c}} \right)^a = \text{sinc}\left(\frac{f}{f_c}\right)^a \quad (4.5)$$

where:

MTFFit(f) = Fitting curve for the MTF

f = spatial frequency

f_c = cutoff frequency

a = fitting parameter

For the specific set of data collected for the AGA 780 in the configuration without polarizer, the best value for "a" was 1.17. Figure 4.4 also shows the fitting curve.

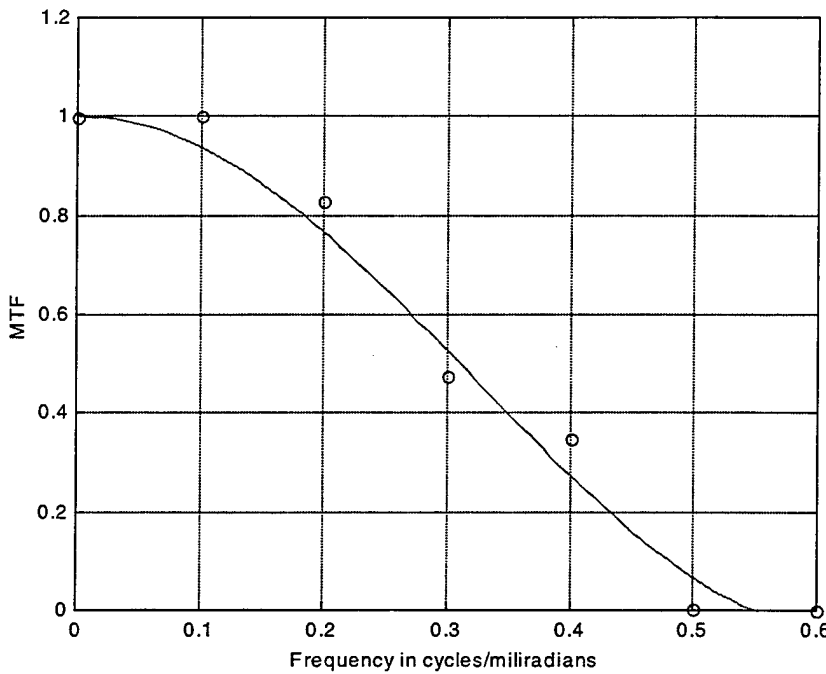


Figure 4.4 – MTF of the AGA 780 (no polarizer) Fitted with the “sinc” Function of Equation 4.4.

D. AGA MRTD

1. Unpolarized Case

Using Matlab® to calculate and plot the MRTD from Equation 3.27 using known or estimated AGA parameters for the unpolarized case, we obtained the curve shown in Figure 4.5. Table 4.2 shows all the values used in this calculation with their respective sources (when available) or the rationale for their estimation.

Parameter	Value	Unit	Source/Rationale
SNR _T	6.5	-	In order to have a probability of detection close to 100%.
D	0.055	m	Operating Manual
D*	4.13e10	Cm Hz ^{1/2} W ⁻¹	Calculated from the given NET
N	1	-	Operating Manual
η_{sc}	0.75	-	Typical value
τ_o	0.7	-	Typical value
α	1.1	mrad	Operating Manual
β	1.1	mrad	Operating Manual
MTF _{system}	-	-	Measured in the laboratory
L	7	-	Standard pattern was used
T _e	0.2	s	Typical value given by Shumaker [Ref. 8, page 8-38]
$\frac{\partial N}{\partial T}$	6.27e-5	(watt cm ⁻² K ⁻¹ sr ⁻¹)	Shumaker [Ref. 8, page 2-36]
FOV _x	7	Degrees	Operating Manual
FOV _y	7	Degrees	Operating Manual

Table 4.2 - MRTD Parameters with no Polarizer. "Most Appropriate" Set Evaluated for the AGA 780.

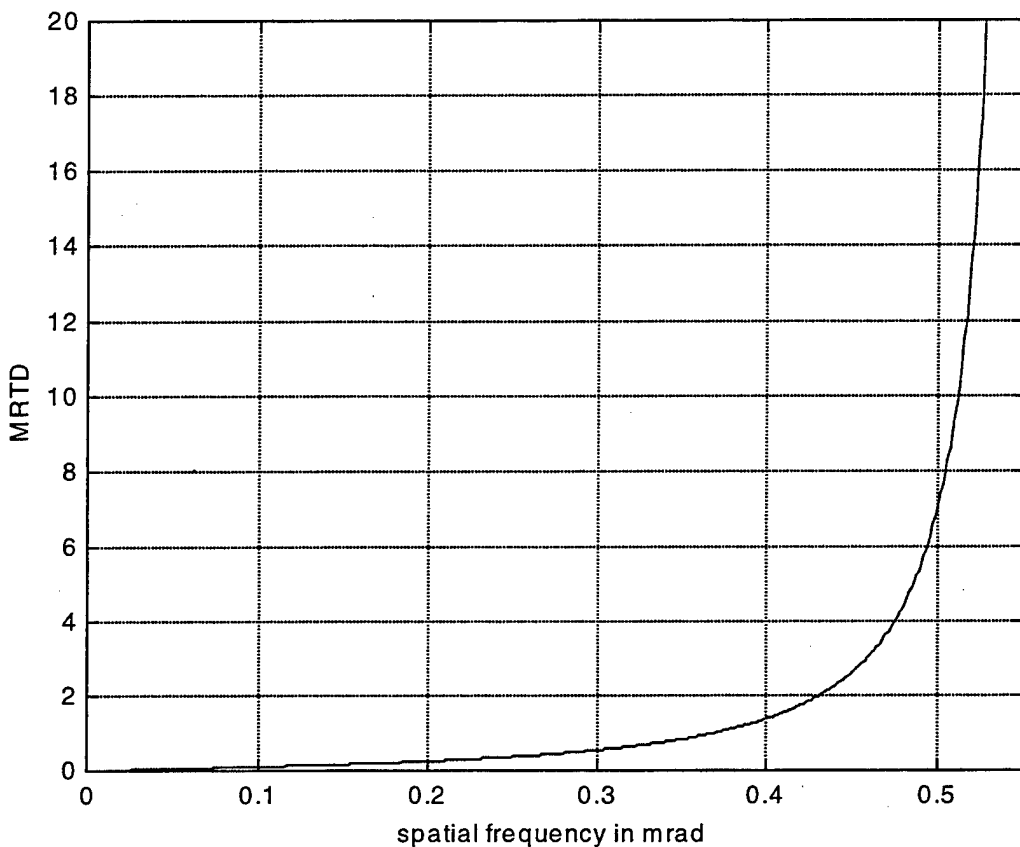


Figure 4.5 - AGA 780 MRTD (Unpolarized case) Based on Estimated Parameters Shown in Table 4.2.

2. Polarized Case

For the polarized case, the same procedure was adopted, except that a new set of data for the MTF was taken, and the formula for the MRTD calculation was modified as shown in Equation 3.32. Table 4.3 shows the new values used in the calculation of the MRTD for the polarized case, with their respective sources (when available) or the rationale for their estimation.

Parameter	Value	Unit	Source/Rationale
SNR _T	6.5	-	In order to have a probability of detection close to 100%.
D	0.055	m	Operating Manual
D*	4.13e10	Cm Hz ^{1/2} W ⁻¹	Calculated from the given NET
N	1	-	Operating Manual
η_{sc}	0.75	-	Typical value
τ_o	0.7	-	Typical value
τ_p	0.85	-	Polarizer specification
α	1.1	mrad	Operating Manual
β	1.1	mrad	Operating Manual
MTF _{polarizer}	-	-	Estimated from the measured MTF of the system with the polarizer
L	7	-	Standard pattern was used
T _e	0.2	s	Typical value given by Shumaker [Ref. 8, page 8-38]
FOV _x	7	Degrees	Operating Manual
FOV _y	7	Degrees	Operating Manual
k	0.5	-	Blackbody approximation
$\frac{\partial N}{\partial T}$	4.00e-5	(watt cm ⁻² K ⁻¹ sr ⁻¹)	Matlab® program dNdT (Appendix A)
T	262	°K	Shumaker [Ref. 8, 2-36]

Table 4.3 - MRTD_p Parameters. The Shading Indicates the Changed Parameters in Relation to Table 4.2.

The plot of the MRTD for the polarized case in comparison to the unpolarized configuration is presented in

Figure 4.6. As expected, the curve representing the system with the polarizer was shifted upwards.

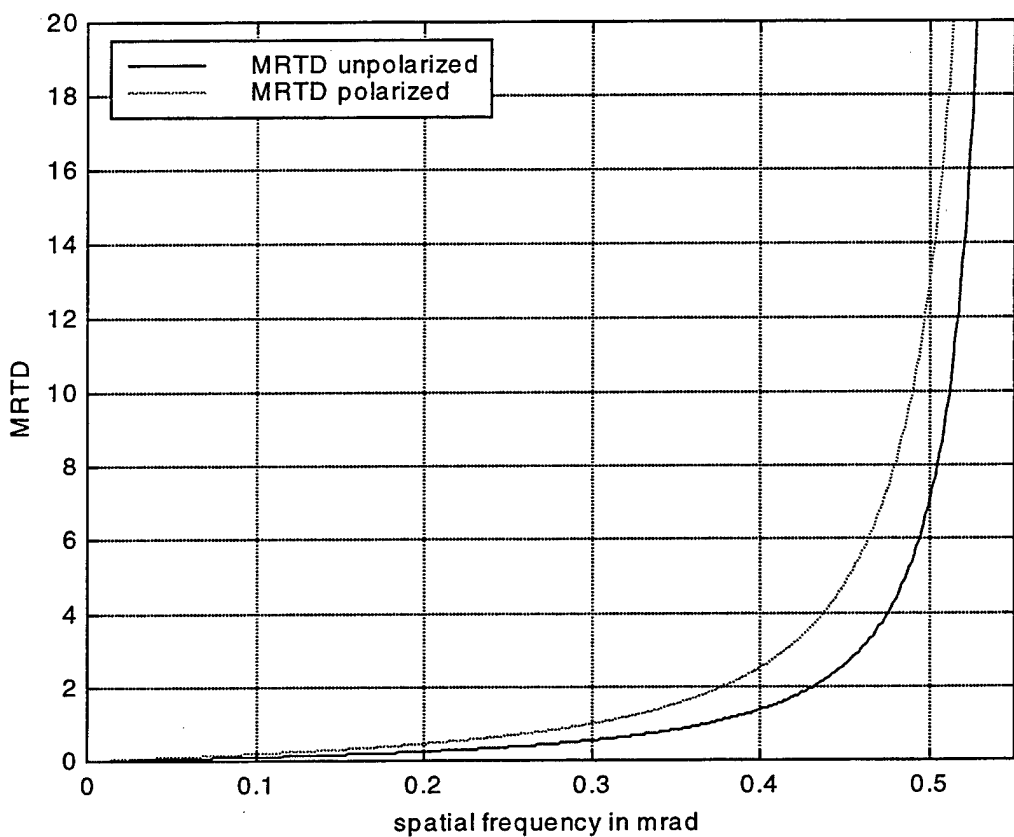


Figure 4.6 - AGA 780 MRTD (Polarized vs. Unpolarized).
Comparison of the $MRTD_p$ Computed from Parameters of Table 4.3
with MRTD from Table 4.2.

V. ANALYSIS OF THE RESULTS

A. THE RESOLUTION PROCESS

While the preliminary data measurements were being taken in the laboratory, some characteristics of the process of resolving a four-bar pattern for the MRTD measurements turned out to be very interesting. Some of them inspired the study of the dynamics of this process and the results derived from this part of the work will be briefly discussed in this section.

The question to be answered when measuring the MRTD is at what point is the four-bar pattern actually seen as a four-bar pattern. Since it is a subjective decision, some factors have great influence on the outcome:

- How well "trained" is the observer?
- What is the dynamic of the experiment? (Does temperature rise in discrete steps and it can be stabilized at a precise value?)
- Is there any delay between the time at which the observer identifies the four-bar pattern and the value is recorded?

- What are the similarities among the recorded images of the objects at the MRTD?

The transition between an unresolved pattern and a "barely" resolved one should be fully understood in order to make sure the value being read is the actual MRTD. The general shape of the MRTD can be illustrated by Figure 5.1 (compare with Figure 4.5). The figure is divided into four basic regions.

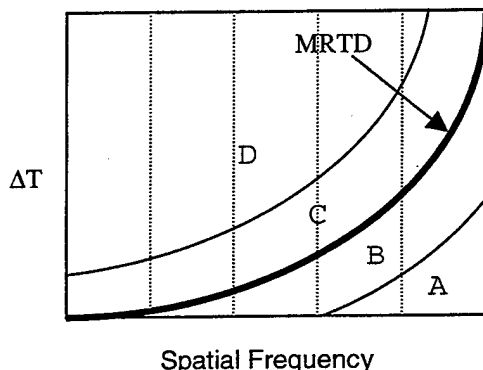


Figure 5.1 - MRTD General Shape and Parameter Space Regions.
Temperature Difference (ΔT) Unresolved.
Temperature Difference Detectable but not Resolvable.
Temperature Difference Resolvable but Operator Dependent.
Temperature Clearly Resolved.

Region A identifies the parameter pairs (spatial frequency and temperature difference) for which the target (four-bar pattern) can not be resolved, mainly because of the effect of the Modulation Transfer Function causing attenuation at the higher frequencies. Region B represents

the pairs which are not yet resolved by the observer, although thorough analysis of the output would reveal that the four-bar characteristic is present. However, the temperature difference between peaks and valleys (Figure 5.2) in the image is less the minimal temperature difference that the system (operator included) can discern. Region C represents a region where MRTD measurements taken by different observers or the same observer in different circumstances may fall. It is easy to notice that it would be extremely difficult to establish a monotonic and smooth line to represent the MRTD by laboratory measurements in which the subjectiveness of the human operator interpretation plays an important role. Finally, region D corresponds to well resolved images (low frequency/high temperature difference pairs).

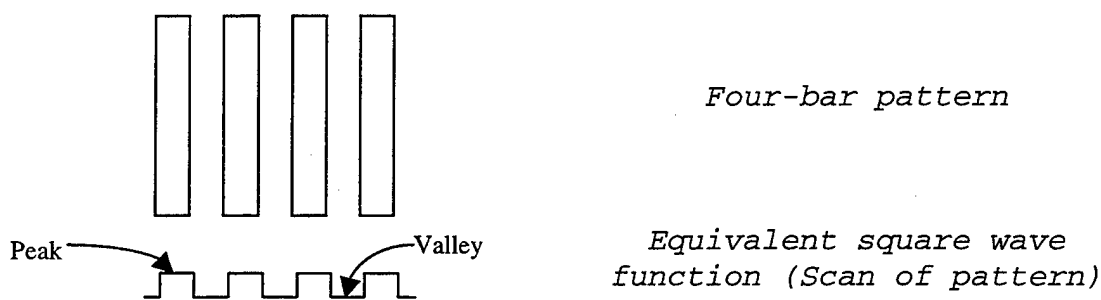


Figure 5.2 - Four-bar Pattern (Peaks and Valleys) with "in-scan" Irradiance Profile.

Output examples of the four regions can be viewed in Figure 5.3, which represents a simulation run in Matlab® (sim_mrt2.m, Appendix A). The region of most interest in this study is of course the boundary between regions B and C (MRTD), and especially region C, where most of the measurements are expected to be found. The next section will propose a method for calibrating values in the region C, so that they can better represent the actual MRTD, and will be standardized between observers.

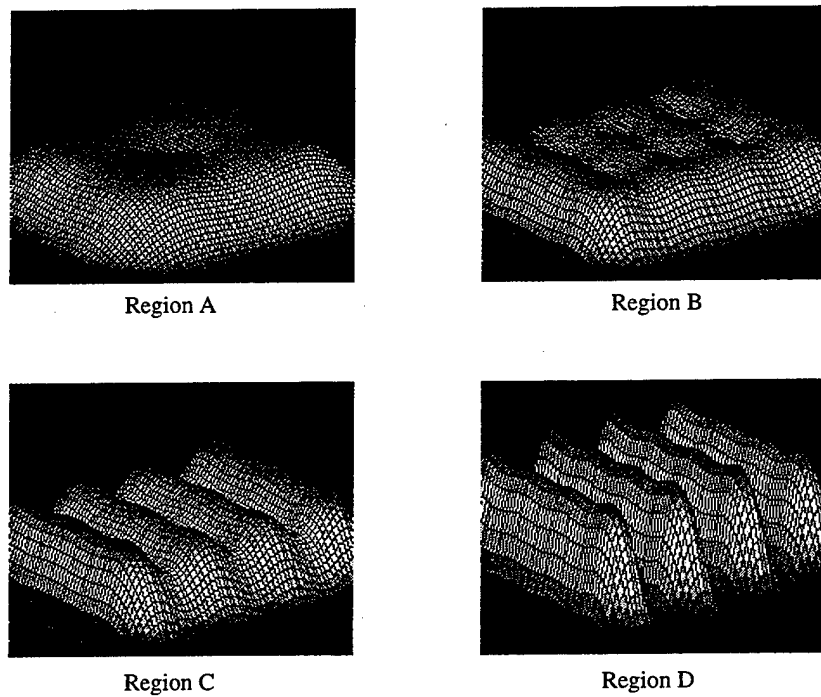


Figure 5.3 – Region A Represents an Unresolved Spatial Frequency. In Region B, the Four-Bar Structure is Present, but the Operator can not Resolve the Bars. Regions C and D Show Well Resolved Spatial Frequencies.

B. A PROPOSED METHOD OF CALIBRATION

As explained in the previous section, region C is of great importance since many of the measurements will be taken there. The main reasons are the psychophysics of the human recognition process and the dynamics of the experiment. The solution proposed to reduce these effects and make use of the measurements taken in region C is to establish a standard output that would be considered an optimum MRTD measurement. Analyses were done on several MRTD data sets and the conclusion reached was that the observer would detect the four-bar pattern as soon as the temperature difference between the peaks and valleys in the output was equal to the minimal discernable temperature of the system. Figure 5.4 shows the output of an ideal MRTD measurement. Notice that the temperature difference between valleys and peaks is approximately 0.1°C , which is the minimal discernable temperature for the AGA 780 [Ref. 4]. It is important to notice that the usual situation is of $T_t > T_b$, hot target against cool background - or "white hot." The situation chosen in this analysis ($T_b < T_t$) represents a reversed contrast, and was chosen due to the simplicity of representing it in the laboratory.

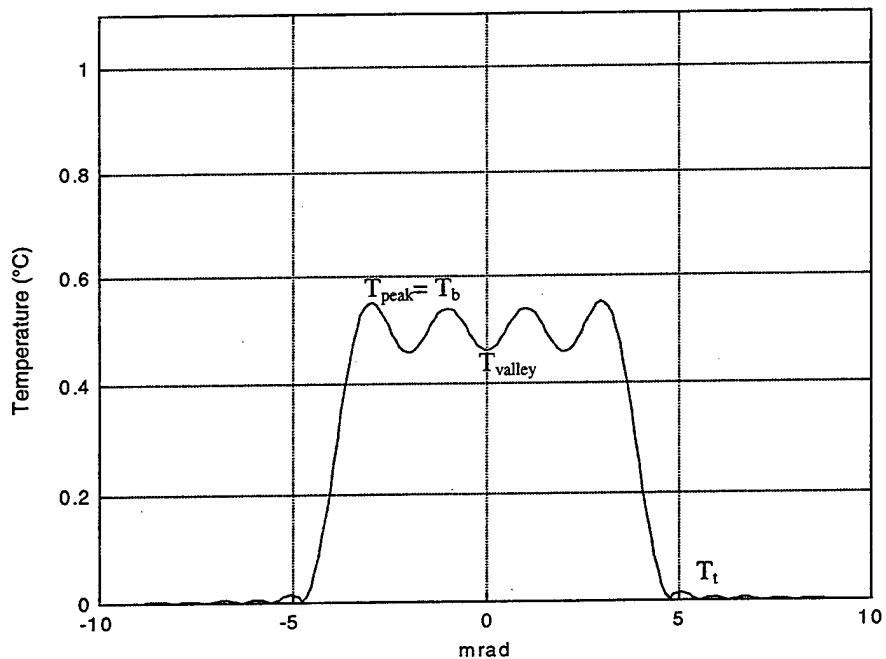


Figure 5.4 - Ideal MRTD Measurements. Detected Signal vs. Angular Position, Scan Direction.

In Figure 5.4, we have:

T_t = target temperature

T_b = background temperature

T_{valley} = apparent temperature in the valley

T_{peak} = apparent temperature of the peak

Based on this "ideal" output and the observation of the typical output falling in region C, we can establish a relationship between those values. By doing so, we "calibrate" the MRTD measurements in region C to more

accurate values. This calibration is illustrated in Figure 5.5.

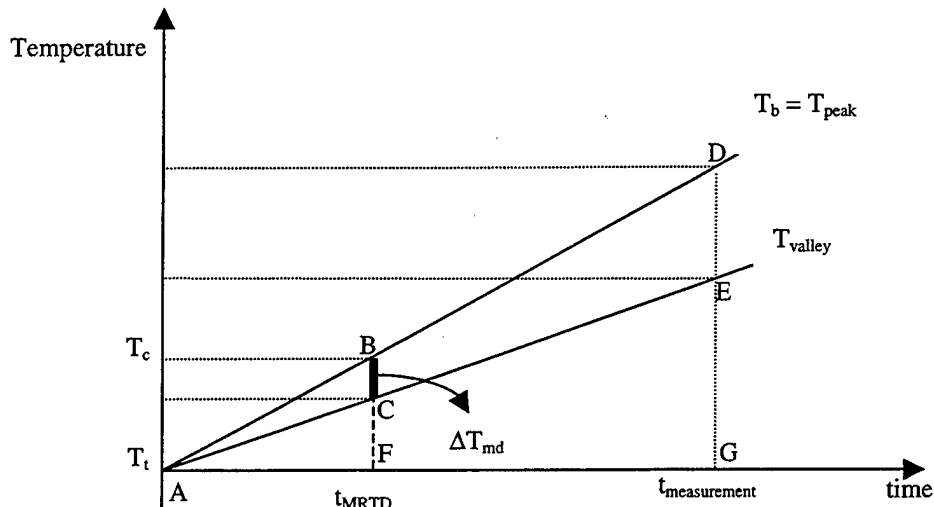


Figure 5.5 - Calibration Process for Observed MRTD. The Value of $t_{\text{measurement}} - t_{\text{MRTD}}$ Corresponds to the Time Lag between Ideal and Non-Ideal Measurements.

The experiment was done so that the target temperature was held constant and the background temperature was increased, and the observer would determine when the four-bar pattern would be just resolved. A delay in determining the actual instant when the MRTD was reached would lead to a measurement falling in region C, which has a greater value of T_b and T_{valley} . In addition, the difference between T_b and T_{valley} is greater than the minimum discernable temperature (T_{md}).

Using properties of similar triangles we can derive a formula for T_c (calibrated temperature). Since triangles ABC and ADE are similar,

$$\frac{DE}{BC} = \frac{DG}{BF} \Rightarrow \frac{T_b - T_v}{\Delta T_{md}} = \frac{T_b - T_t}{T_c - T_t} \quad (5.1)$$

from which

$$T_c = \frac{\Delta T_{md} \cdot (T_b - T_t) + T_t \cdot (T_b - T_v)}{(T_b - T_v)} \quad (5.2)$$

so that

$$MRTD_{cal} = T_c - T_t = \frac{\Delta T_{md} \cdot (T_b - T_t)}{T_b - T_v} \quad (5.3)$$

where:

ΔT_{md} = minimum discernable temperature

T_c = calibrated background temperature

$MRTD_{cal}$ = calibrated MRTD.

Figure 5.6 shows a comparison between a data set taken by an untrained observer and the corresponding calibrated version. As a reference, the calculated value of the MRTD is also included. The uncalibrated data show considerable scatter, with a "fitted" value that deviates widely from

the calculated MRTD. The "calibrated" data however show much reduced scatter and a fitted value in much closer agreement with the calculation. For the trained observer the measured and calibrated data show very close agreement. This means that the trained observer is much more likely to determine the exact moment when the four-bar pattern is just resolvable. Figure 5.7 shows an equivalent data set to that of 5.6, but taken by a trained observer. Although Figures 5.6 and 5.7 also represent different polarization filters, it will not affect the analysis of the improvement in quality of the data collected from a trained observer.

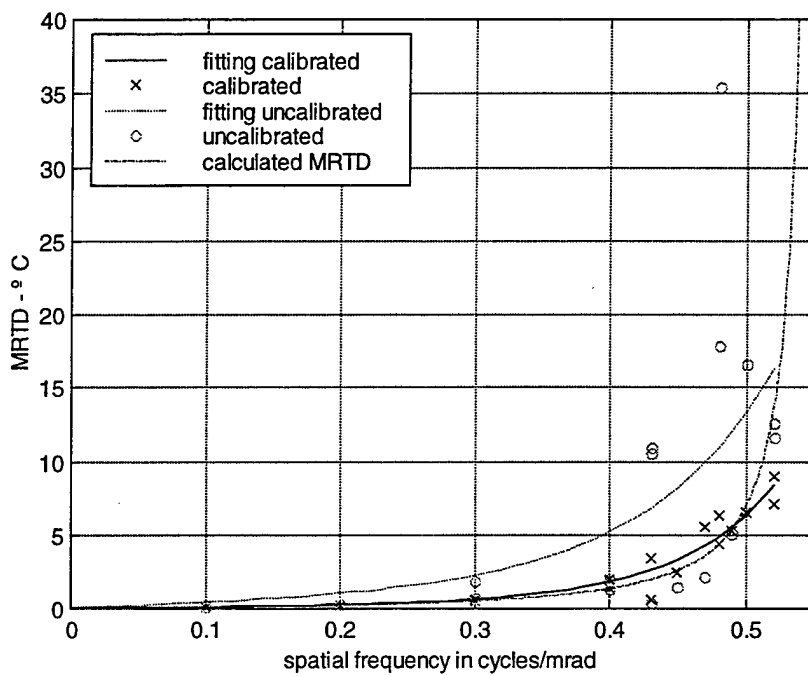


Figure 5.6 - Comparison of Uncalibrated, Calibrated and Calculated MRTD (Untrained Observer - Unpolarized Case).

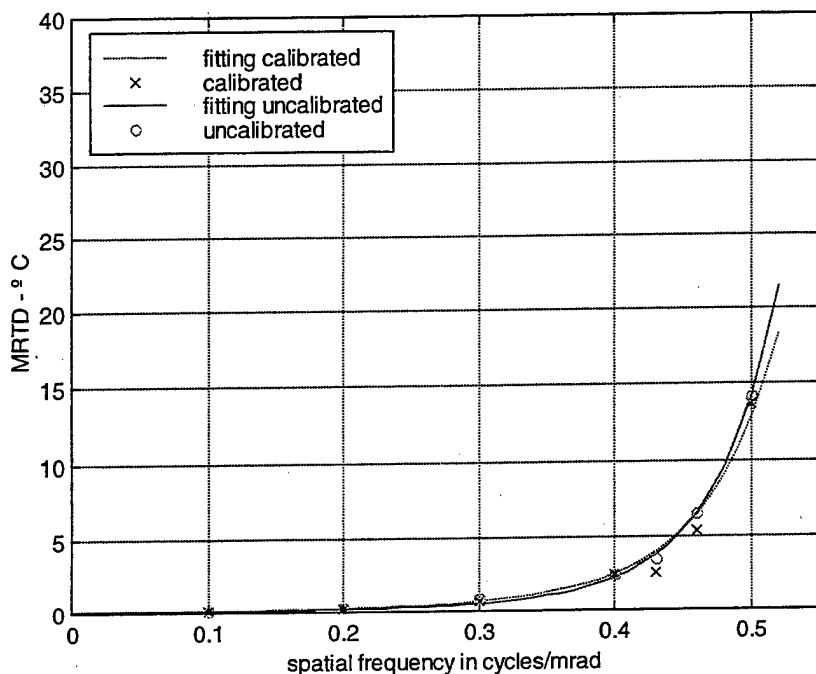


Figure 5.7 - Comparison of Uncalibrated and Calibrated MRTD for a Trained Observer (Vertical Polarization Filter).

C. CALCULATED DATA VERSUS MEASURED DATA

After collecting the laboratory data, the next step was to verify how close the measured values were to the calculated ones. Using the MRTD developed in Chapter III and the parameters in Tables 4.2 and 4.3, we compared calculated and measured data. Figure 5.8 shows the comparison for the unpolarized case. In this case, three sets of data were taken in different days (May 5th, 11th, and 25th). We can observe the scatter decreasing with repetition of the task, with the third set (May 25th) corresponding to

the trained observer, showing very little scatter and excellent agreement with the calculation.

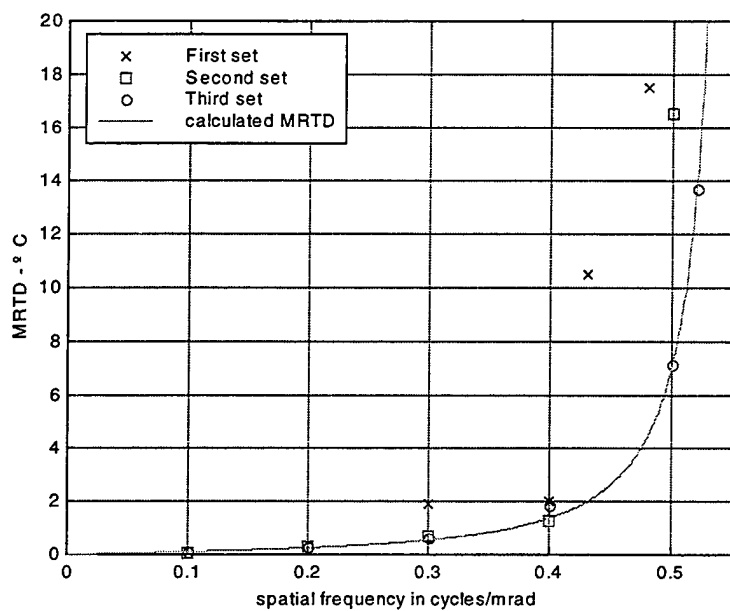


Figure 5.8 - Comparison of Measured and Calculated MRTD (Unpolarized Case), and Influence of Training.

X: Measurement of May 5;
: Measurement of May 11;
O: Measurement of May 25.

Figures 5.9 and 5.10 show equivalent comparisons to data of Figure 5.8 but taken using polarization filters. Filters 4 and 5 correspond to the horizontal and vertical polarization filters respectively. In both plots, the comparison is made between "trained observer" data and the calculated $MRTD_p$.

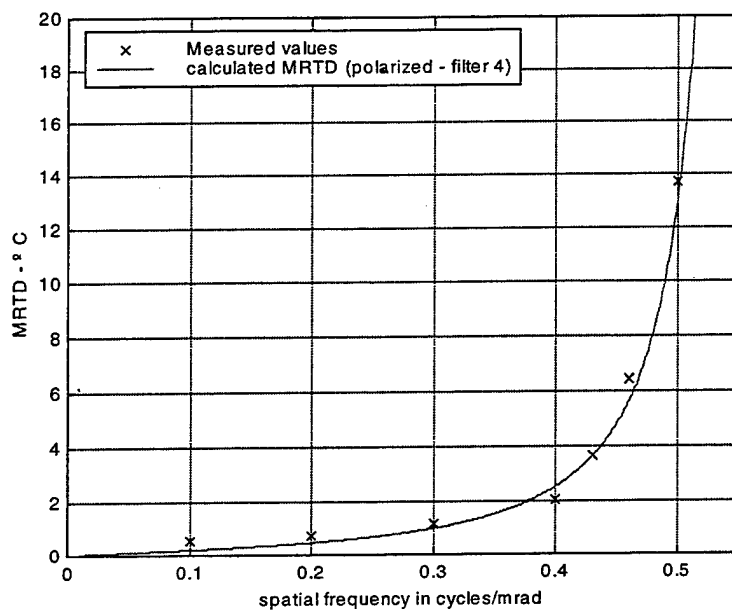


Figure 5.9 - Comparison of Measured and Calculated MRTD_p, (Horizontal Polarization Case - Filter 4).

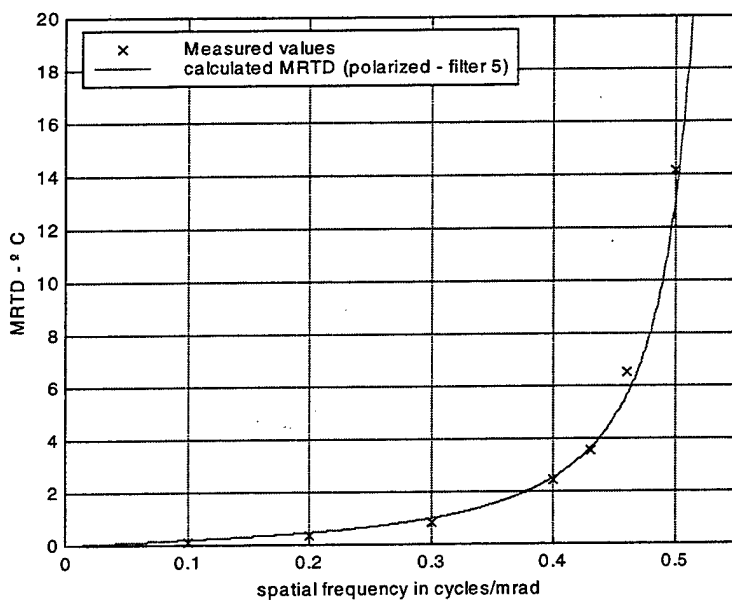
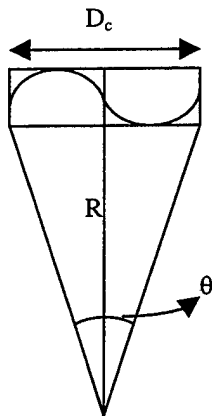


Figure 5.10 - Comparison of Measured and Calculated MRTD_p, (Vertical Polarization Case - Filter 5).

D. RANGE CALCULATION

The final analysis in this thesis is the range calculation. The maximum range at which some specific task can be performed is estimated using the apparent target-background temperature difference (TBTD) and the MRTD curves, developed in Chapter III. Although MRTD is a function of spatial frequency, we can translate it into a function of range, if specific target and task are given. Some criteria have been established to relate the resolution of bar charts to levels of visualization [Ref. 8]. Johnson [Ref. 10] first suggested his criteria in 1957. Others such as Moser and O'Neill followed him with their own criteria. Basically, all the criteria try to establish the number of resolution elements (resels) or line pairs per critical dimension needed to perform a given task. It is then possible to convert spatial frequency into distance, as seen in Figure 5.11. It is important to notice that one spatial cycle corresponds to two resels. We need then to have a full cycle of spatial frequency on the average target dimension being observed to achieve detection. This dimension is also known as "critical dimension," and is defined differently by various authors.



$$\begin{aligned}
 2 \text{ resels} &= 1 \text{ cycle} \\
 \theta &= 2 \cdot \text{Angle of Subtense} \\
 f &= \frac{1}{\theta} \\
 \theta &\approx \frac{D_c}{R}
 \end{aligned}$$

Figure 5.11 - Conversion of Spatial Frequency into Distance (Task: Detection).

Using the small angle approximation, and applying the appropriate factor to get the result in cycles per milliradians, we have the following formula:

$$R = \frac{2000 D_c f}{N} \quad (5.4)$$

where:

R = Range (m).

D_c = Critical Dimension (m).

f = spatial frequency (cycles/mrad).

N = Number of resels per critical dimension (D_c), based on some pre-established criteria. For example, N would be equal to two for detection.

Figure 5.12 shows the unpolarized and polarized MRTD developed in Chapter III plotted as a function of range for detection (two resolution elements in the critical dimension) of a target with critical dimension of 15m (comparable to the Research Vessel "POINT SUR" used in the EOPACE³ campaign).

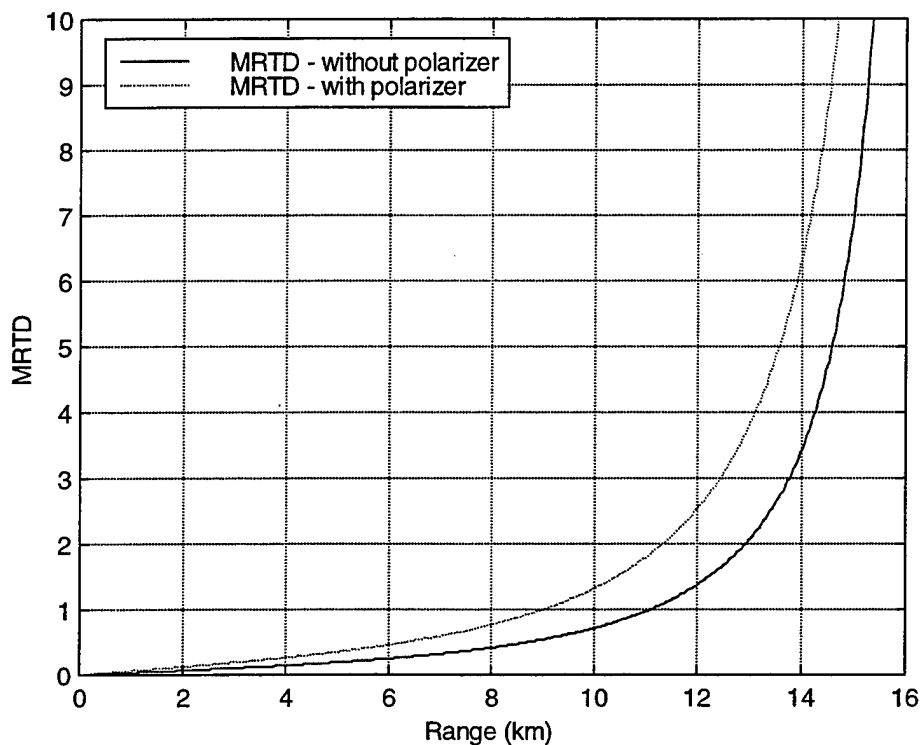


Figure 5.12 - MRTD for the AGA 780 as a Function of Range (Polarized and Unpolarized Cases)

³ EOPACE - Electro Optic Propagation Assessment in the Coastal Environment was a multinational measurement series in San Diego Bay in 1996, sponsored by ONR, and organized by SPAWAR SYSTEMS CENTER. Its overall purpose was to quantify infrared (IR) propagation characteristics for near ocean surface transmission and analyze electro-optic (EO) systems performance in the coastal environment condition [Ref. 12]

Now, it is necessary to model the second part of the problem, the apparent temperature difference as a function of range. The main interest of this thesis is in the maritime environment, where the sea surface emission (background) near the Brewster angle in the 8-12 μ m region has been shown to exhibit strong vertical polarization [Ref. 1]. By using a horizontal polarizer, it is possible to filter out some of the background radiation, thus improving the contrast.

The observed degree of polarization of the radiance is defined as [Ref. 1]:

$$POL = \frac{\langle N_v \rangle - \langle N_h \rangle}{\langle N_v \rangle + \langle N_h \rangle} \quad (5.5)$$

where:

$\langle N_v \rangle$ = mean apparent vertically polarized radiance.

$\langle N_h \rangle$ = mean apparent horizontally polarized radiance.

It means that a degree of polarization greater than zero implies a net vertical polarization, while zero corresponds to an unpolarized source. Table 5.1 tabulates the percentages of vertical and horizontal polarization corresponding to some values of POL. The mathematical analysis involved in this table is carried out in

Equations 5.6 to 5.12. We define

$$\frac{\langle N_v \rangle}{\langle N_v \rangle + \langle N_h \rangle} \text{ and } \frac{\langle N_h \rangle}{\langle N_v \rangle + \langle N_h \rangle} \quad (5.6)$$

as the fractions of vertical and horizontal polarization radiance. If we subtract those expressions, we have:

$$\frac{\langle N_v \rangle}{\langle N_v \rangle + \langle N_h \rangle} - \frac{\langle N_h \rangle}{\langle N_v \rangle + \langle N_h \rangle} = \frac{\langle N_v \rangle - \langle N_h \rangle}{\langle N_v \rangle + \langle N_h \rangle} = \text{POL} \quad (5.7)$$

which is the same as equation 5.5. Adding the two expressions in 5.6 the result is one.

$$\frac{\langle N_v \rangle}{\langle N_v \rangle + \langle N_h \rangle} + \frac{\langle N_h \rangle}{\langle N_v \rangle + \langle N_h \rangle} = \frac{\langle N_v \rangle + \langle N_h \rangle}{\langle N_v \rangle + \langle N_h \rangle} = 1 \quad (5.8)$$

We then have a system with two equations and two unknowns:

$$\frac{\langle N_v \rangle}{\langle N_v \rangle + \langle N_h \rangle} - \frac{\langle N_h \rangle}{\langle N_v \rangle + \langle N_h \rangle} = \text{POL} \quad (5.9)$$

$$\frac{\langle N_v \rangle}{\langle N_v \rangle + \langle N_h \rangle} + \frac{\langle N_h \rangle}{\langle N_v \rangle + \langle N_h \rangle} = 1 \quad (5.10)$$

Solving the system above for the fractions of vertical and horizontal polarization radiance, we have

$$\frac{\langle N_v \rangle}{\langle N_v \rangle + \langle N_h \rangle} = \frac{(1 + \text{POL})}{2} \quad (5.11)$$

$$\frac{\langle N_h \rangle}{\langle N_v \rangle + \langle N_h \rangle} = \frac{(1 - \text{POL})}{2} \quad (5.12)$$

POL	Percent Vertical polarization	Percent Horizontal polarization
0	50%	50%
0.1	55%	45%
0.2	60%	40%
0.3	65%	35%
POL	$(1+POL)/2$	$(1-POL)/2$

Table 5.1 - Degrees of Polarization and Respective Percentages.

Typical values for the degree of sea polarization measured during the MAPTIP⁴ campaign range from 7 to 30% in the LWIR band. Assuming the target is unpolarized (POL=0), we can use a horizontally polarized filter to eliminate some of the background radiation. Knowing target and background temperatures, we can calculate the mean radiance at zero range (Equations 2.5 and 3.2). A perfect horizontally polarizing filter would eliminate 50% of the target radiance and $(1+POL)/2$ of the background radiance (see Table 5.1). Since only a fraction of the total radiance is passing, the sensor "sees" the scene as if the target and background both had lower temperatures. It means that the observed temperature is smaller than the emitted. The observed temperature can be calculated by solving Equation 3.28 for T_B , when "k" is equals to the

⁴ MAPTIP - Marine Aerosol Properties and Thermal Imager Performance Trial campaign was held in coastal waters of Katwijk, Netherlands, in 1993. Its objective was "to improve marine aerosol models for the marine boundary layer and the modeling of electromagnetic propagation and imaging in the coastal environment." [Ref. 1]

fraction of the total radiance passing through the filter, in this case $(1-POL)/2$. An apparent target-background temperature difference (TBTD) at zero range can then be established.

Table 5.2 shows some values of apparent TBTD for the case where target temperature (T_T) is 310° and background temperature (T_B) is 300°K . Appendix D shows a table of values for $\langle N \rangle$ for temperatures ranging from 240 to 320°K .

POL	7%	10%	20%	30%
$\langle N_T \rangle$ (310°)	$1.1278\text{e-}3$	$1.1278\text{e-}3$	$1.1278\text{e-}3$	$1.1278\text{e-}3$
$\langle N_B \rangle$ (300°)	$9.6243\text{e-}4$	$9.6243\text{e-}4$	$9.6243\text{e-}4$	$9.6243\text{e-}4$
$\langle N_T' \rangle$ with polarizer	$5.639\text{e-}4$	$5.639\text{e-}4$	$5.639\text{e-}4$	$5.639\text{e-}4$
$\langle N_B' \rangle$ with polarizer	$4.4753\text{e-}4$	$4.3309\text{e-}4$	$3.8497\text{e-}4$	$3.3685\text{e-}4$
T_T'	270.4°K	270.4°K	270.4°K	270.4°K
T_B'	259.2°K	257.7°K	252.4°K	246.7°K
ΔT (unp.)	10°	10°	10°	10°
$\Delta T'$ (pol.)	11.2°	12.7°	18°	23.7°

Table 5.2 - Calculation of Apparent TBTD as a Function of the Degree of Polarization of the Background with Unpolarized Target.

In Table 5.2, the following parameters are shown:

$\langle N_T \rangle$ = mean emitted target radiance.

$\langle N_B \rangle$ = mean emitted background radiance.

$\langle N_T' \rangle$ = mean observed target radiance ($\langle N_T \rangle * 0.5$).

$\langle N_B' \rangle$ = mean observed background radiance ($(\langle N_B \rangle * (1-POL)/2)$).

T_T' = apparent target temperature (from Equation 3.28).

T_B' = apparent background temperature (from Equation 3.28).

ΔT = actual temperature difference (310° - 300° K).

$\Delta T'$ = observed temperature difference ($T_T' - T_B'$).

The next step is to calculate the apparent temperature as a function of range, using a computer code that estimates atmospheric transmittance, such as LOWTRAN, MODTRAN, or SEARAD. A Matlab program (rangeimp.m - Appendix A) was written to calculate and plot the MRTD and the apparent TBTD versus range for the example presented in this section. This program takes the apparent temperature difference shown in Table 5.2 and multiplies it by a transmissivity factor obtained from SEARAD for the following set of input parameters:

- Lowtran7 was selected.
- Type of atmospheric path: Slant path between two altitudes.
- Surface albedo of earth: assumed blackbody.
- Navy maritime model.
- No clouds or rain.
- Altitude of the target: 0.
- Altitude of the sensor: 300ft.
- Wind speed: 7.5 m/s.

- Wind speed: 7.5 m/s (24h average).
- Airmass character: 3.
- Visibility: the program calculated visibility from the standard data for the chosen conditions (Mid-latitude summer).

Figures 5.13 and 5.14(zoom) show the result of this calculation, which is summarized in Table 5.3. Figure 5.13 shows the apparent TBTD computed for various degrees of polarization as a function of range for the sample atmospheric conditions. The MRTD for detection with and without the polarizer is plotted on the same scale for an assumed 15m target critical dimension. For any case the intersection of corresponding TBTD and MRTD curves defines the detection range. Figure 5.14 shows a magnified plot of the intersection region of Figure 5.13.

We can observe that for degrees of polarization greater than 20% we obtain an improvement in range by using the polarizing filter. On the other hand, values of POL smaller than 20% imply degraded range performance, since the effects of the polarizer in increasing MRTD are more significant than the improvement in the apparent TBTD.

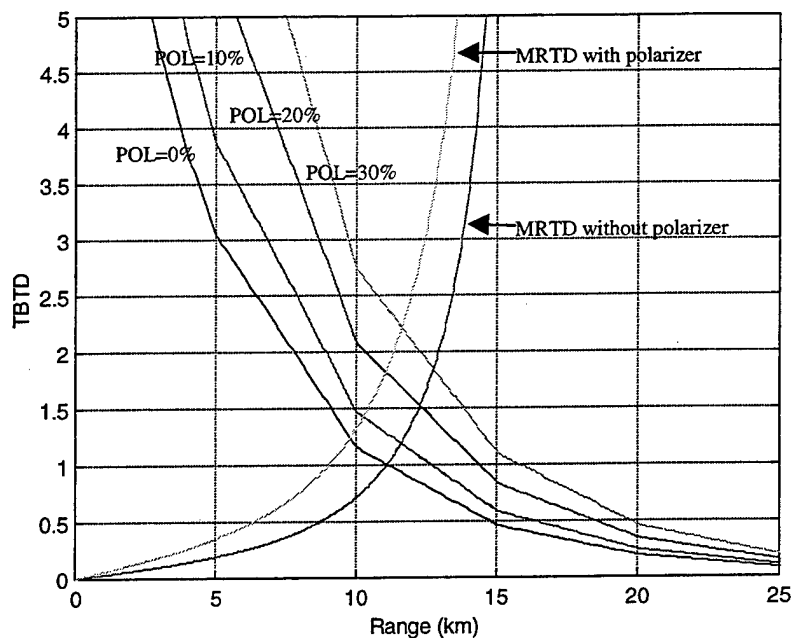


Figure 5.13 – MRTD and TBTD as Functions of Range, for Various Degrees of Polarization. MRTD is for Detection with Critical Dimension 15m. Intersection Points Define Maximum Ranges for Detection.

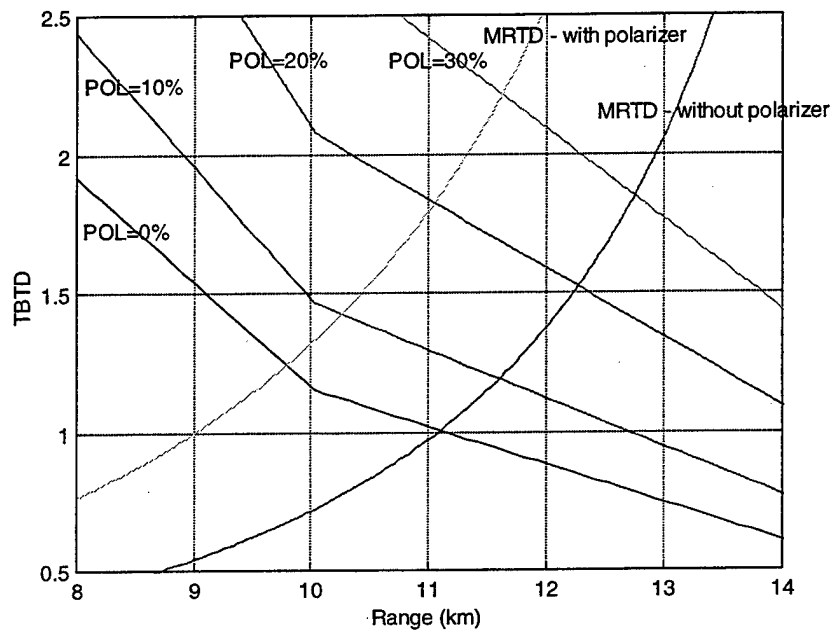


Figure 5.14 – MRTD and TBTD as Functions of Range (Zoom).

POL	Range (km)	Difference (km)
0%	11.13	0
10%	10.25	-0.88
20%	11.06	-0.07
30%	11.63	0.60

Table 5.3 – Difference in Range Performance for Increasing Degrees of Polarization.

All the calculation done so far approximates the real world, since it assumes a simple model where only the radiance from target and background are accounted for. More elaborate models have been proposed, such as the one shown in Lagaras [Ref. 11], which uses experimental data from the EOPACE campaign. In his work, Lagaras suggested a TBTD for both cases, with and without polarization, using target temperature of 300.26°K and background temperature of 289.95°K , as shown in Figure 5.15.

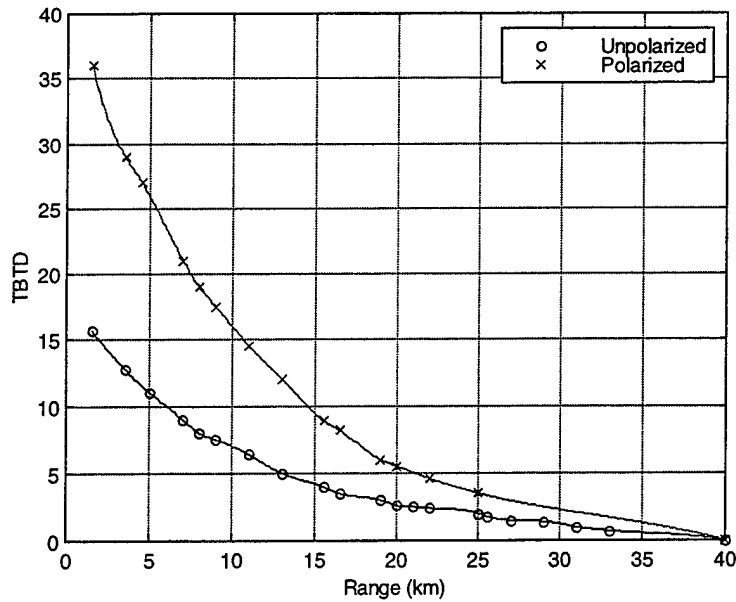


Figure 5.15 - TBTD for Polarized and Unpolarized Cases [After Ref. 11].

Comparing this new set of TBTD curves and our formulation for the MRTD for both cases, we notice a small improvement in range, as shown in Figure 5.16.

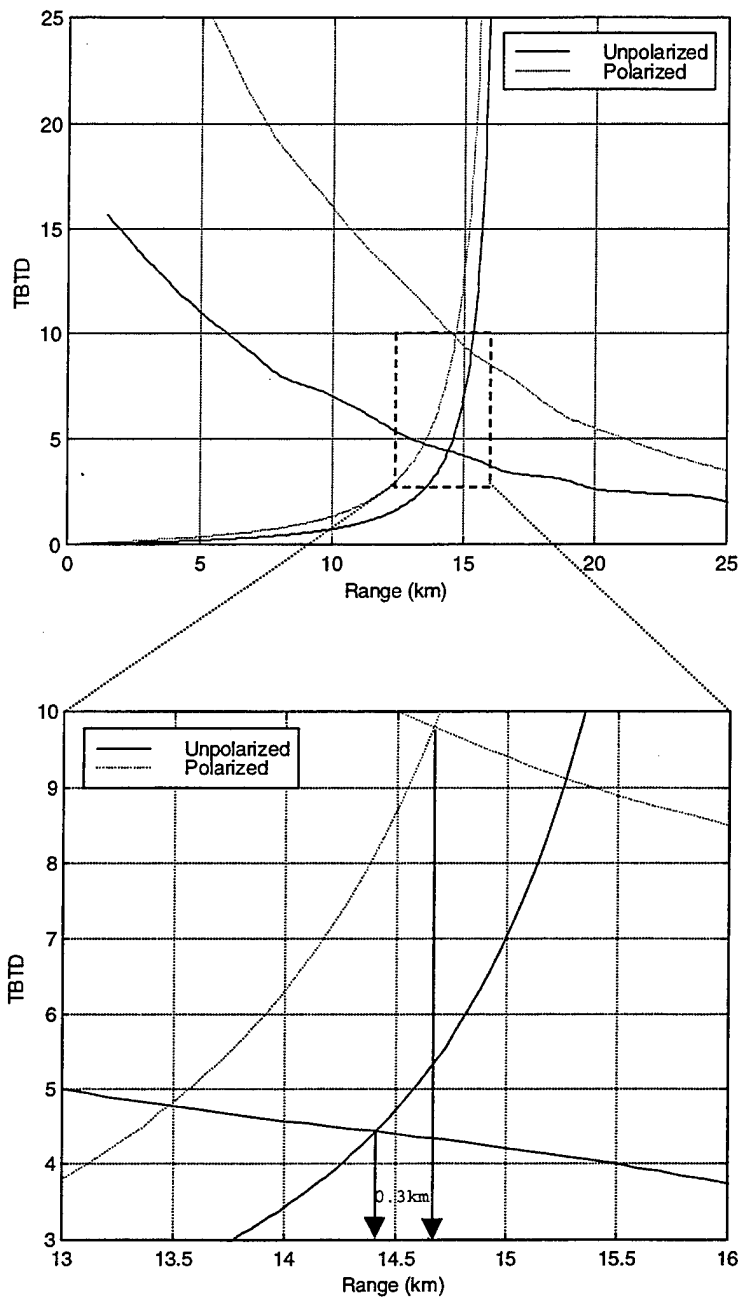


Figure 5.16 - MRTD and TBTD as Functions of Range.

Both results presented in Figures 5.14 and 5.16 show that it is possible to achieve some improvement in range

performance for thermal imaging systems. However the results also pointed out to a relatively small improvement, if any. It should be noted that the calculations were made for only a single target critical dimension, a single atmosphere state, and two TBTD cases.

VI. CONCLUSION

The main objective of this thesis was to determine a more appropriate Minimum Resolvable Temperature Difference (MRTD) formulation for use with a polarization filtered thermal imaging system (generic FLIR). In order to analyze the problem, two approaches were used.

First, a mathematical formulation was derived from the traditional MRTD expressions used by various authors [Ref. 8 and Ref. 9]. Polarization filter transmissivity, Modulation Transfer Function (MTF), and the "thermal derivative" of Planck's Equation were studied and their effects introduced to the new MRTD formulation, when applicable. In a second phase, laboratory experiments using the AGA Thermovision 780 system were conducted. The MRTD patterns were set up (see Appendix B) with the object of gathering data to be compared to the proposed mathematical formulation.

The main conclusions of this work are listed below:

- The mathematical formulation suggests that use of polarization filters increases the temperature difference at which the observer detects the four-bar pattern. This reduction in performance depends

on the polarization filter characteristics as well as on the new reference temperature to be used in the "thermal derivative" of Planck's Equation.

- The experimental data agreed with the mathematical formulation. Data collected in the laboratory showed very small deviation from the proposed MRTD developed in this thesis. Figure 6.1 summarizes both the results of the mathematical formulation and the laboratory results.

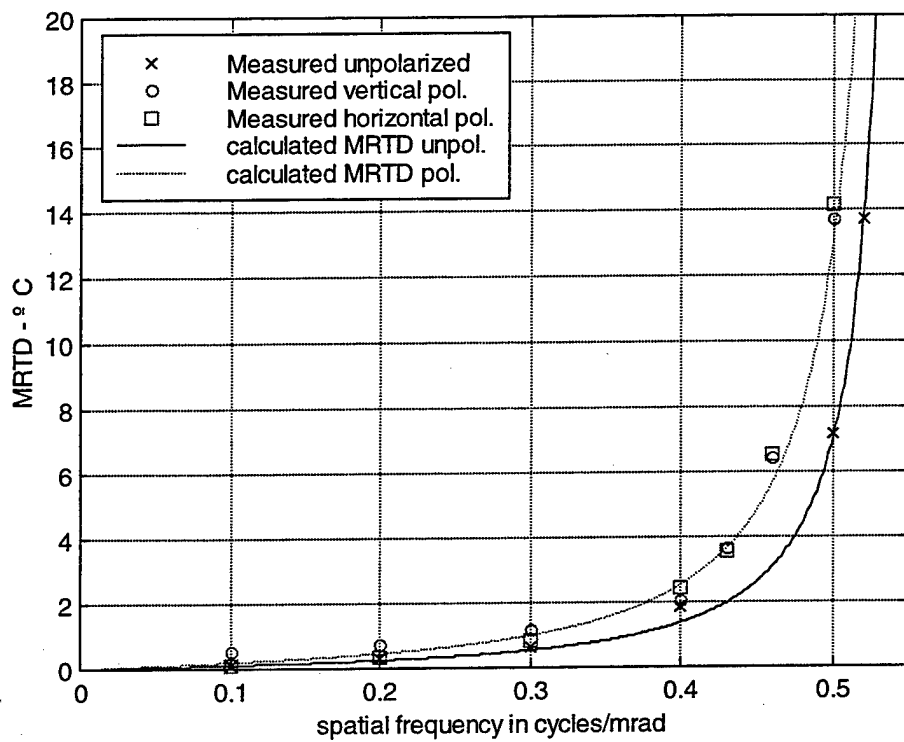


Figure 6.1 - Summary of Mathematical and Experimental Values of MRTD with and without Polarizing Filters.

- The process of resolving the four-bar pattern (or any type of target) is very complex. Training plays a decisive role in the ability to determine the exact MRTD value. In Chapter IV, a calibration method was proposed to adjust measurements taken by an untrained observer or under non-ideal conditions. The use of this method would enable the untrained observer to attain results comparable to the better-trained one.
- Range calculation suggested that the use of polarization filters might improve the performance of thermal imaging systems in a marine environment, under certain conditions. The main factor to be determined is the degree of polarization of the sea surface. A high degree of polarization would lead to an improvement in range. On the other hand, low degrees of polarization would imply degradation of the system performance. The example used in this research showed improvement in range when the degree of polarization was greater than 20%.

It is important to emphasize that this work is not self-contained. Extensive work was previously done in

collecting field data as well as modeling the target and the background [Ref. 1, 11, 12, 13, and 14]. There are still some aspects to be analyzed or improved. As a suggestion for future work, it would be interesting to refine the target-to-background temperature models. It would allow better range improvement calculations. In addition, more precise laboratory measurements would help to validate the mathematical formulation proposed here. This would be necessary to have a temperature-controlled laboratory, with precise instruments, and an adequate number of trained observers.

The results of this work, added to the results of others in this area, may be useful in improving the performance of thermal imaging systems. The expected improvement margin, though not large, may be enough to help systems with limited range capability. Moreover, tactical decision assessment for electro-optic systems operating in a marine environment should include results of this work. It would allow them to achieve higher effectiveness when assessing decisions over situations where the maximum possible performance is expected.

APPENDIX A. MATLAB SOURCE CODES

The following Matlab codes are presented in this Appendix:

FILE NAME	CHAPTER OF REFERENCE
fig2_2.m	II
fig2_3.m	II
fig4_3.m	IV
mtffit.m	IV
mrtd_plot.m	IV
sim_mrt2.m	V
dl2temp.m	V
plotcal.m	V
plotcal5.m	V
fig5_8.m	V
fig5_9.m	V
fig5_10.m	V
dndt.m	V
Enne.m	V
Rangeimp4.m	V
Rangeimp5.m	V
Fig6_1.m	VI
readptw2.m	IV ⁵
readmtf.m	IV ⁶
filt.m	IV ⁷
guil.m	IV ⁸
readgui.m	IV ⁹

Table A.1 - List of Matlab® Programs.

⁵, ⁶, ⁷, ⁸, and ⁹ - those programs were not referenced in Chapter IV, but were used to analyze most of the results collected during the experiments discussed in that chapter.

```

%***** ****
%***** Naval Postgraduate School - CA ****
%***** Thesis Research ****
% Type : Procedure
% Name : fig2_2
% Function: plots Planck's Equation for four different
% temperatures and shows Wien's Law
% Date : Jul / 1999
% Version : 1.0
% Author : Edson Fernando da Costa Guimaraes, Capt. (BAF)
% Routine Information:
% 1) calculates Planck's Equation for T=220, 250, 280,
%    300, 320°K
% 2) plots the results
%***** ****
%***** ****
clear
close all
lambda=0:0.01:25;

% Planck's Equation for T=220
T0=220;
c1=3.7418e4;
c2=1.4388e4;
M0=exp(c2./(lambda*T0))-1;
M1=(c1./(lambda.^5));
M220=M1./M0;

% Planck's Equation for T=250
T1=250;
M2=exp(c2./(lambda*T1))-1;
M250=M1./M2;

% Planck's Equation for T=280
T2=280;
M3=exp(c2./(lambda*T2))-1;
M280=M1./M3;

% Planck's Equation for T=300
T3=300;
M4=exp(c2./(lambda*T3))-1;
M300=M1./M4;

% Planck's Equation for T=320

```

```

T4=320;
M5=exp(c2./(lambda*T4))-1;
M320=M1./M5;

% Wien's Displacement Law
l0=2897/T0;
l1=2897/T1;
l2=2897/T2;
l3=2897/T3;
l4=2897/T4;
L=[l0,l1,l2,l3,l4]
maxima=[max(M220),max(M250),max(M280),max(M300),max(M320)];

% plots the results
figure(1)
plot(lambda,M250,lambda,M280,lambda,M300,lambda,M320, L,
maxima,':')
grid on
gtext('250 K')
gtext('280 K')
gtext('300 K')
gtext('320 K')
xlabel('Wavelength - micrometer')
ylabel('Spectral Radiant Exitance - M')

%***** Naval Postgraduate School - CA *****
%***** Thesis Research *****

% Type      : Procedure
% Name      : fig2_3
% Function: plots transmissivity data from Searad
% Date      : May / 1999
% Version   : 1.0
% Author    : Edson Fernando da Costa Guimaraes, Capt. (BAF)
% Routine Information:
%     1) plots the data collected from Searad
%***** Midlatitude summer *****
%***** Horizontal path 1Km *****

```

```

% Navy Maritime Aerosol
% Airmass Characteristic = 3
% No clouds, no rain
% Sea Level
% Temperature of the boundary = 300K

% lambda = wavelength vector from 2 to 20μm
lambda=[20.000 19.231 18.519 17.857 17.241 16.667 16.129
15.625 15.152 14.706 14.286 13.889 13.514 13.158 12.821
12.500 12.195 11.905 11.628 11.364 11.111 10.870 10.638
10.417 10.204 10.000 9.804 9.615 9.434 9.259 9.091 8.929
8.772 8.621 8.475 8.333 8.197 8.065 7.937 7.813 7.692 7.576
7.463 7.353 7.246 7.143 7.042 6.944 6.849 6.757 6.667 6.579
6.494 6.410 6.329 6.250 6.173 6.098 6.024 5.952 5.882 5.814
5.747 5.682 5.618 5.556 5.495 5.435 5.376 5.319 5.263 5.208
5.155 5.102 5.051 5.000 4.950 4.902 4.854 4.808 4.762 4.717
4.673 4.630 4.587 4.545 4.505 4.464 4.425 4.386 4.348 4.310
4.274 4.237 4.202 4.167 4.132 4.098 4.065 4.032 4.000 3.968
3.937 3.906 3.876 3.846 3.817 3.788 3.759 3.731 3.704 3.676
3.650 3.623 3.597 3.571 3.546 3.521 3.497 3.472 3.448 3.425
3.401 3.378 3.356 3.333 3.311 3.289 3.268 3.247 3.226 3.205
3.185 3.165 3.145 3.125 3.106 3.086 3.067 3.049 3.030 3.012
2.994 2.976 2.959 2.941 2.924 2.907 2.890 2.874 2.857 2.841
2.825 2.809 2.793 2.778 2.762 2.747 2.732 2.717 2.703 2.688
2.674 2.660 2.646 2.632 2.618 2.604 2.591 2.577 2.564 2.551
2.538 2.525 2.513 2.500 2.488 2.475 2.463 2.451 2.439 2.427
2.415 2.404 2.392 2.381 2.370 2.358 2.347 2.336 2.326 2.315
2.304 2.294 2.283 2.273 2.262 2.252 2.242 2.232 2.222 2.212
2.203 2.193 2.183 2.174 2.165 2.155 2.146 2.137 2.128 2.119
2.110 2.101 2.092 2.083 2.075 2.066 2.058 2.049 2.041 2.033
2.024 2.016 2.008 2.000];;

% t = transmissivity vector for lambda
t=[0.0025 0.0045 0.0180 0.0310 0.0310 0.0504 0.0342 0.0027
0.0000 0.0000 0.0103 0.1287 0.2467 0.4353 0.5171 0.5290
0.6542 0.6792 0.7016 0.7259 0.7611 0.7658 0.7870 0.7856
0.7985 0.8166 0.7890 0.7828 0.7765 0.8055 0.7911 0.7857
0.7615 0.7369 0.6692 0.6575 0.5460 0.4979 0.2434 0.1874
0.1375 0.0256 0.0083 0.0006 0.0000 0.0000 0.0000 0.0000
0.0000 0.0000 0.0000 0.0000 0.0000 0.0000 0.0000 0.0000
0.0000 0.0000 0.0000 0.0000 0.0000 0.0000 0.0000 0.0000
0.0000 0.0000 0.0000 0.0000 0.0003 0.0029 0.0054 0.0073
0.0365 0.0912 0.2170 0.2216 0.2948 0.4341 0.4646 0.5111
0.6017 0.6619 0.6706 0.7095 0.6769 0.4922 0.3929 0.2232

```

```

0.0921 0.0249 0.0001 0.0000 0.0000 0.0000 0.0002 0.7085
0.7962 0.8291 0.8592 0.8782 0.8972 0.8992 0.8795 0.8603
0.8365 0.8390 0.8202 0.7925 0.7776 0.7961 0.8043 0.6836
0.7986 0.7778 0.7328 0.7102 0.7125 0.7548 0.7826 0.7804
0.7662 0.7536 0.6786 0.5842 0.4220 0.3888 0.2501 0.3650
0.2384 0.2441 0.1095 0.0745 0.4278 0.5665 0.3040 0.2678
0.1270 0.1496 0.1740 0.1286 0.2060 0.2595 0.3180 0.1514
0.2103 0.1939 0.1510 0.0780 0.0620 0.0228 0.0036 0.0007
0.0001 0.0000 0.0000 0.0000 0.0000 0.0000 0.0000 0.0000
0.0000 0.0000 0.0000 0.0000 0.0000 0.0000 0.0000 0.0000
0.0000 0.0000 0.0000 0.0000 0.0001 0.0037 0.0357 0.1192
0.1256 0.2859 0.4405 0.4001 0.5262 0.5733 0.5078 0.6329
0.6640 0.6633 0.7131 0.7682 0.7613 0.8134 0.8317 0.8473
0.8596 0.8581 0.8802 0.8827 0.8818 0.8913 0.8935 0.8982
0.8908 0.8844 0.8477 0.8566 0.8429 0.8672 0.8609 0.8502
0.8919 0.9017 0.8840 0.8620 0.8741 0.8509 0.8541 0.8371
0.7984 0.7479 0.7332 0.7881 0.8184 0.8024 0.7187 0.5597
0.5325 0.5743 ];
subplot(6,1,[1,2,3,4,5])
plot(lambda, t)
grid
xlabel('wavelength - micrometer')
ylabel('Transmissivity')
axis([2,20,0,1])

```

```

%***** Naval Postgraduate School - CA *****
%***** Thesis Research *****

% Type      : Procedure
% Name      : fourier2
% Function: compares input and output for a given spatial
%            frequency
% Date      : Jul / 1999
% Version   : 1.0
% Author    : Edson Fernando da Costa Guimaraes, Capt. (BAF)
% Routine Information:
%   1) inputs the spatial frequency
%   2) calculates the pattern
%   3) process the input (MTF)
%   4) plots input and output
%*****
```

```

clear
close all
points=1000;
mn=-50;
mx=50;
mrad=linspace(mn,mx,points);

% gets MTF from MTFFit function
MTFFit;
close all

% builds a two-side MTF
MTF2=[fliplr(MTF1) MTF1];
MTF3=zeros(1,length(mrad));
MTF3((length(mrad)/2-length(MTF2)/2
+1):(length(mrad)/2+length(MTF2)/2))=MTF2;

% inputs data
f=input('Enter the spatial frequency:');
cycle=1/f;

% builds the pattern
pat1=zeros(1,length(mrad));
unit=cycle*points/(mx-mn);
L=3.5*unit;
warning off
s=-cos(mrad*2*pi/cycle);
s(find(s>=0))=1;
s(1:(length(mrad)-L)/2)=0;
s(((length(mrad)-L)/2)+L+1):length(mrad))=0;
s(find(s<0))=0;
warning on

% FFT of the pattern
S=fft(s);
freq1=0.5*length(mrad)/(mx-mn);
freq=linspace(-freq1,freq1,length(mrad));
figure(1)
subplot(2,1,2)
S=fftshift(S);

% "convolution"
OUT=MTF3.*S;
out=ifft(OUT);

```

```

% plots the results
figure(1)
subplot(1,2,1)
plot(mrad,s)
grid
axis([-2*cycle 2*cycle 0 1.1])
subplot(1,2,2)
plot(mrad,abs(out))
grid
axis([-2*cycle 2*cycle 0 1.1])

%***** Naval Postgraduate School - CA *****
%***** Thesis Research *****
% Type : Procedure
% Name : mtffit
% Function: fits a curve to the MTF data
% Date : Jul / 1999
% Version : 1.0
% Author : Edson Fernando da Costa Guimaraes, Capt. (BAF)
% Routine Information:
%    1) plots the data collected from the AGA
%    2) fits the data to a 'sinc' function
%***** *****
%***** *****
%clear
% MTF measured data
mean0=[66.5592 64.5289];
mean1=[66.5809 64.5434];
mean2=[65.1908 63.5347];
mean3=[65.7399 64.7775];
mean4=[64.9921 64.2948];
mean5=[65.5592 65.5520];
mean6=[65.5520 65.5520];

% calculates modulation
f=[0 0.1 0.2 0.3 0.4 0.5 0.6];
m0=(mean0(1)-mean0(2))/(mean0(1)+mean0(2));
m1=(mean1(1)-mean1(2))/(mean1(1)+mean1(2));
m2=(mean2(1)-mean2(2))/(mean2(1)+mean2(2));
m3=(mean3(1)-mean3(2))/(mean3(1)+mean3(2));
m4=(mean4(1)-mean4(2))/(mean4(1)+mean4(2));

```

```

m5=(mean5(1)-mean5(2))/(mean5(1)+mean5(2));
m6=(mean6(1)-mean6(2))/(mean6(1)+mean6(2));
m=[m0 m1 m2 m3 m4 m5 m6];
MTF=m/max(m);

% fitting process
min=1e10;
ER=[];
for x=1:0.01:2
    MTF_fit=(sinc(f/(.55))).^x;
    err2=sum((MTF_fit-MTF).^2);
    if err2<min
        min=err2;
        ER=[ER err2];
        m=[x];
    end
end

% plots the results
f1=linspace(0,0.55,55);
MTF1=(sinc(f1/(.55))).^m(1);

figure(1) % this is figure 4.4 in chapter IV
plot(f,MTF,'o',f1,MTF1,'m')
grid
xlabel('Frequency in cycles/miliradians')
ylabel('MTF')
axis([0 0.6 0 1.2])

%*****
%***** Naval Postgraduate School - CA *****
%***** Thesis Research *****
% Type      : Procedure
% Name      : mrtd_plot
% Function: calculates and plots MRTD
% Date      : Jul / 1999
% Version   : 1.0
% Author    : Edson Fernando da Costa Guimaraes, Capt. (BAF)
% Routine Information:
%     1) calculates MRTD (unpolarized case)
%     2) calculates MRTD (polarized case)
%     3) plots the results

```

```

%*****
%*****
%clear all
% AGA 780 data (unpolarized case)
SNRT=6.5; % use 2.5 if only 50%Pd is required ;
deltax=1.1; % in-scan detector subtense (mRad);
deltay=1.1; % cross-scan detector subtense in
(mRad);
L=7; % length to width ratio of the MRTD
bar;
te=0.1; % eye integration time (s);
Fr=6.25; % frame rate (Hz);
Nos=1; % overscan ratio;
Nss=1; % serial scan ratio;
FOVx=(7*pi/180)*1000; % in-scan field-of-view (mRad);
FOVy=(7*pi/180)*1000; % cross-scan field-of-view (mRad);
F=0.20; % focal length (m);
tau0=0.6; % transmission of the optics;
Nd=1; % number of detectors;
Nsc=0.75; % scan efficiency;
D=0.055; % aperture (m)
Deestar=4.12866e10; % detectivity (cm-Hz^(1/2)-watt(-1) =
(calculated from NET)
dndT=6.27e-5; % derivative of Planck's Equation
(relative to 300°K)

% NET calculation
NET_numerator=20*F*(FOVx*FOVy*Fr*Nos*Nss)^(0.5);
NET_denominator=tau0*((pi*Nd*Nsc).^(0.5))*(D^2)*deltax*delt
ay*Deestar*dndT;
NET=NET_numerator/NET_denominator;

% spatial frequency
f0=linspace(0,0.55,400);

% noise filter factor calculation
rb=0.335; %
rox=(1+(2*f0*rb).^2).^(-0.5);

% fitting curve to allow better interpolation
MTFFfit=(sinc(f0/.55)).^1.17;

% MRTD calculation

```

```

MRTD_300=2*SNRT*NET*(1./MTFFit).*((rox).^0.5).*((((f0).^2)*
deltax*deltay/L).^0.5)*(te*Fr*Nos*Nss).^-0.5;

% polarized case (T=262)
taup=0.85; % transmission of the polarizer
dndT=4.00e-5; % derivative of Planck's Equation
(relative to 262°K)

% NET calculation
NET_numerator=20*F*(FOVx*FOVy*Fr*Nos*Nss)^0.5;
NET_denominator=taup*tau0*((pi*Nd*Nsc).^(0.5))*(D^2)*deltax
*deltay*Deestar*dndT;
NET=NET_numerator/NET_denominator;

% MRTD calculation
MRTD_pol=2*SNRT*NET*(1./MTFFit).*((rox).^0.5).*((((f0).^2)*
deltax*deltay/L).^0.5)*(te*Fr*Nos*Nss).^-0.5;

% plots the results
figure(3)
plot(f0,MRTD_300,f0,MRTD_pol,:')
xlabel('spatial frequency in mrad')
ylabel('MRTD')
axis([0 0.55 0 20])
legend('MRTD unpolarized', 'MRTD polarized',2)
grid

% zoom
figure(4)
plot(f0,MRTD_300,f0,MRTD_pol,:')
xlabel('spatial frequency in mrad')
ylabel('MRTD')
axis([0.3 0.55 0 12])
legend('MRTD unpolarized', 'MRTD polarized',2)
grid

%*****
%***** Naval Postgraduate School - CA *****
%***** Thesis Research *****
% Type : Procedure
% Name : sim_mrt2
% Function: simulates mrtd measurements
% Date : May / 1999

```

```

% Version : 1.0
% Author  : Edson Fernando da Costa Guimaraes, Capt. (BAF)
% Routine Information:
%   1) creates a four bar pattern
%   2) creates a simulated output for regions A, B, C, and
%      D, as explained in figure 5.1 in chapter V.
%*****
%*****
clear

% creates a four-bar pattern
m=zeros(250,256);
factor=8;
a=factor*7;
bar=ones(a,factor);

m(128-factor*3.5+1:128+factor*3.5,125-factor*3.5+1:125-
factor*3.5+factor)=bar;
m(128-factor*3.5+1:128+factor*3.5,125-
factor*3.5+1+2*factor:125-factor*3.5+2*factor+factor)=bar;
m(128-factor*3.5+1:128+factor*3.5,125-
factor*3.5+1+4*factor:125-factor*3.5+4*factor+factor)=bar;
m(128-factor*3.5+1:128+factor*3.5,125-
factor*3.5+1+6*factor:125-factor*3.5+6*factor+factor)=bar;

% calculates the pattern fft
f2=fft2(m);
f2=fftshift(f2);

a=[9 14 15 19]; % scales the model to have outputs in
regions A, B, C, and D
for y=1:4
b=ones(a(y),a(y));
for i=1:a(y)
  for j=1:a(y)
    b(i,j)=(-i^2-j^2);
  end
end
b1=b;
b2=fliplr(b);
b3=flipud(b);
b4=flipud(b2);
BB=[b4 b3;b2 b1];

```

```

BB=BB+abs(BB(1));
BB=BB/max(max(BB));
B=zeros(250,256);
B(125-a(y)+1:125+a(y),128-a(y)+1:128+a(y))=BB;

% multiplies pattern FFT and modeled MTF
test=f2.*B;
test2=ifft2(test);

% plots the results
figure(1) % this is figure 5.3 in chapter V
subplot(2,2,y)
surf(abs(test2))
axis([100,150,100,150, 0 1])
axis off
end

%*****
%***** Naval Postgraduate School - CA *****
%***** Thesis Research *****
% Type : Function
% Name : dl2temp
% Function: converts digital level to temperature
% Date : Jul / 1999
% Version : 1.0
% Author : Edson Fernando da Costa Guimaraes, Capt. (BAF)
% Routine Information:
% 1) inputs:
%     a) digital level
%     b) thermal level
%     c) thermal range
%     d) polarization filter number
% 2) output:
%     a) temperature in degrees centigrades
%*****
%***** function tempC=dl2temp(dl,tl,tr,p)
if dl<=4095 & dl>=0
    if tl>=0 & tl<=1000
        if tr==2 | tr==5 | tr==10 | tr==20 | tr==50 | tr==100
        | tr==200 | tr==500 | tr==1000

```

```

% transforms digital level in isothermal units
iu=dl*tr/4095+tl-tr/2;
% transforms isothermal units in temperature
switch p
    case 0
        A=2318; B=1218; C=0.742;
    case 4
        A=5.679; B=57.46; C=0.918;
    case 5
        A=5.679; B=57.46; C=0.918;
    end
    tempK=B/(log((A+iu)/(C*iu)));
    %temperature in Kelvin
    tempC=tempK-273.15; %temperature in Celcius
else
    error('Thermal Range must be 2, 5, 10, 20, 50,
100, 200, 500, or 1000')
end
else
    error('Thermal Level must be a integer between 0 and
1000')
end
else
error('Digital level must be a integer between 0 and 4095')
end

if tl<tr/2
    warning('This combination of thermal range and thermal
Level may result in complex valued calculations')
end

%***** Naval Postgraduate School - CA *****
%***** Thesis Research *****
% Type      : Procedure
% Name      : plotcal
% Function: compares calibrated and uncalibrated data
(filter 0)
% Date      : Jul / 1999
% Version   : 1.0
% Author    : Edson Fernando da Costa Guimaraes, Capt. (BAF)
% Routine Information:
%     1) plots the data collected from the AGA

```

```

% 2) fits the data
% 3) plots the calibrated data
% 4) plots the calculated MRTD
%***** ****
%***** ****
clear

% measrued data
f=[0.1 0.2 0.3 0.3 0.4 0.4 0.43 0.43 0.43 0.45 0.47 0.48
0.48 0.49 0.5 0.52 0.52];
MRT=[0.1 0.3 1.9 0.7 2 1.3 0.4 10.9 10.5 1.5 2.1 35.4 17.9
5.1 16.6 11.6 12.6];

% calibrated data (using procedure proposed in chapter IV)
MRTcal=[0.076277651 0.192184497 0.465116279 0.568643379
1.958863859 1.352757544 0.539811066 3.367315416 3.37403599
2.396166134 5.540897098 6.307911618 4.341498909 5.290456432
6.566455696 7.16934487 9.01932713];

% fitting process
%net=0.12;
%das=1.1;
%SL=0.075*net;
%SC=1.3*net*das;
%ER=1;
min=1e10;
ER=[];
for B=0.6:0.01:0.8
    for C=10:0.01:12
        MRTD=0.05+B*f.*exp(C*f.^2);
        err2=sum((MRTD-MRTcal).^2);
        if err2<min
            min=err2;
            ER=[ER err2];
            m=[B C];
        end
    end
end
min=1e10;
for B1=0:0.1:4
    for C1=0:0.1:20
        MRTD1=0.05+B1*f.*exp(C1*f.^2);
        err2=sum((MRTD1-MRT).^2);
        if err2<min

```

```

        min=err2;
        ER=[ER err2];
        m1=[B1 C1];
    end
end

% spatial frequency
f1=0:0.01:0.52;

% result of the fitting process
MRTD=0.05+m(1)*f1.*exp(m(2)*f1.^2);
MRTD1=0.05+m1(1)*f1.*exp(m1(2)*f1.^2);

% gets calculated MRTD from mrtd_plot function
mrtd_plot;
close all

% plots the results
plot(f1,MRTD,f,MRTcal,'x',f1,MRTD1,:',f,MRT,'o',f0,MRTD_30
0,'-.')
legend('fitting calibrated','calibrated','fitting
uncalibrated','uncalibrated','calculated MRTD',2)
grid
axis([0 0.55 0 40])
xlabel('spatial frequency in cycles/mrad')
ylabel('MRTD - °C')

*****
%***** Naval Postgraduate School - CA *****
%***** Thesis Research *****
% Type : Procedure
% Name : plotcal
% Function: compares calibrated and uncalibrated data
% (filter 5)
% Date : Jul / 1999
% Version : 1.0
% Author : Edson Fernando da Costa Guimaraes, Capt. (BAF)
% Routine Information:
% 1) plots the data collected from the AGA
% 2) fits the data
% 3) plots the calibrated data
*****

```

```

*****  

clear

% measured data
f=[0.1 0.2 0.3 0.4 0.43 0.46 0.5];
MRT=[0.12 0.34 0.84 2.45 3.56 6.56 14.16];
MRTcal=[0.07138608 0.214105793 0.717335611 2.437810945
2.51590106 5.324675325 13.69439072];

%fitting process
%net=0.12;
%das=1.1;
%SL=0.075*net;
%SC=1.3*net*das;
%ER=1;
min=1e10;
ER=[];
for B=0.5:0.01:0.8
    for C=10:0.01:30

%MRTD=SL+((SC*2*f)/2.646).*exp(1.571*(ER^2)*(f.^2));
    MRTD=0.05+B*f.*exp(C*f.^2);
    err2=sum((MRTD-MRTcal).^2);
    if err2<min
        min=err2;
        ER=[ER err2];
        m=[B C];
    end
    end
end
min=1e10;
for B1=0:0.1:4
    for C1=0:0.1:40

%MRTD=SL+((SC*2*f)/2.646).*exp(1.571*(ER^2)*(f.^2));
    MRTD1=0.05+B1*f.*exp(C1*f.^2);
    err2=sum((MRTD1-MRT).^2);
    if err2<min
        min=err2;
        ER=[ER err2];
        m1=[B1 C1];
    end
    end
end

```

```

% spatial frequency
f1=0:0.01:0.52;

% result of the fitting process
MRTD=0.05+m(1)*f1.*exp(m(2)*f1.^2);
MRTD1=0.05+m1(1)*f1.*exp(m1(2)*f1.^2);

% plots the results
plot(f1,MRTD,:',f,MRTcal,'x',f1,MRTD1,f,MRT,'o')
grid
axis([0 0.55 0 40])
legend('fitting calibrated','calibrated','fitting
uncalibrated','uncalibrated',2)
xlabel('spatial frequency in cycles/mrad')
ylabel('MRTD - °C')

%***** Naval Postgraduate School - CA *****
%***** Thesis Research *****
% Type : Procedure
% Name : fig5_8a
% Function: plots calculated vs measured MRTD values for
% filter 0 (unpolarized case)
% Date : Jul / 1999
% Version : 1.0
% Author : Edson Fernando da Costa Guimaraes, Capt. (BAF)
% Routine Information:
% 1) calculates MRTD
% 2) plots calculated MRTD vs measured MRTD
%***** *****
%***** measured data (unpolarized)
clear

% first set
f_1=[0.3 0.4 0.43 0.48];
MRT_1=[1.9 2 10.5 17.5];
MRT_1cal=[0.51 1.65 3.20 3.91];

% second set
f_2=[0.1 0.2 0.3 0.4 0.5];
MRT_2=[0.06 0.28 0.67 1.28 16.56];

```

```

MRT_2cal=[0.05 0.17 0.62 1.17 9.07];

% third set
f_3=[0.1 0.2 0.3 0.4 0.5 0.52];
MRT_3=[0.1 0.3 0.64 1.84 7.17 13.72];
MRT_3cal=[0.05 0.17 0.63 2.27 4.86 10.13];

% AGA 780 data (unpolarized case)
SNRT=6.5; % use 2.5 if only 50%Pd is required ;
deltax=1.1; % in-scan detector subtense (mRad);
deltay=1.1; % cross-scan detector subtense in (mRad);
L=7; % length to width ratio of the MRTD bar;
te=0.1; % eye integration time (s);
Fr=6.25; % frame rate (Hz);
Nos=1; % overscan ratio;
Nss=1; % serial scan ratio;
FOVx=(7*pi/180)*1000; % in-scan field-of-view (mRad);
FOVy=(7*pi/180)*1000; % cross-scan field-of-view (mRad);
F=0.20; % focal length (m);
tau0=0.6; % transmission of the optics;
Nd=1; % number of detectors;
Nsc=0.75; % scan efficiency;
D=0.055; % aperture (m)

% detectivity (cm-Hz^(1/2)-watt(-1) = (calculated from NET)
Deestar=4.12866e10;
% derivative of Planck's Equation (relative to 300°K)
dndT=6.27e-5;

% NET calculation
NET_numerator=20*F*(FOVx*FOVy*Fr*Nos*Nss)^(0.5);
NET_denominator=tau0*((pi*Nd*Nsc).^(0.5))*(D^2)*deltax*...
deltay*Deestar*dndT;
NET=NET_numerator/NET_denominator;

% spatial frequency
f0=linspace(0,0.55,400);

% noise filter factor calculation
rb=0.335; %
rox=(1+(2*f0*rb).^2).^(-0.5);

% fitting curve to allow better interpolation
MTFFit=(sinc(f0/.55)).^1.17;

```

```

MRTD_300=2*SNRT*NET*(1./MTFFit).*((rox).^0.5).*(((f0).^2)...
    *deltax*deltay/L).^0.5)*(te*Fr*Nos*Nss).^-0.5;

% plots the results
figure(1)
plot(f_1, MRT_1, 'x', f_2, MRT_2, 's', f_3, MRT_3, ...
    'o', f0, MRTD_300, '-')
legend('First set', 'Second set', 'Third set', 'calculated...
    MRTD', 2)
grid
axis([0 0.55 0 20])
xlabel('spatial frequency in cycles/mrad')
ylabel('MRTD - °C')

%***** Naval Postgraduate School - CA *****
%***** Thesis Research *****
% Type : Procedure
% Name : fig5_9
% Function: plots calculated vs measured MRTD values for
%           filter 4
% Date : Jul / 1999
% Version : 1.0
% Author : Edson Fernando da Costa Guimaraes, Capt. (BAF)
% Routine Information:
%   1) calculates MRTD
%   2) plots calculated MRTD vs measured MRTD
%***** *****
%***** measured data (polarized)
clear

f_1=[0.10 0.20 0.30 0.40 0.43 0.46 0.50 0.52];
MRT_1=[0.5600 0.7200 1.1700 2.0600 3.6700 6.4400 13.7200
40.9500];
MRT_1cal=[0.0974 0.1793 0.7638 1.1012 1.6141 2.6747 5.7369
23.0554];

% AGA 780 data (unpolarized case)
SNRT=6.5;           % use 2.5 if only 50%Pd is required ;
deltax=1.1;          % in-scan detector subtense (mRad);

```

```

deltay=1.1;           % cross-scan detector subtense in (mRad);
L=7;                  % length to width ratio of the MRTD bar;
te=0.1;               % eye integration time (s);
Fr=6.25;              % frame rate (Hz);
Nos=1;                % overscan ratio;
Nss=1;                % serial scan ratio;
FOVx=(7*pi/180)*1000; % in-scan field-of-view (mRad);
FOVy=(7*pi/180)*1000; % cross-scan field-of-view (mRad);
F=0.20;               % focal length (m);
tau0=0.6;              % transmission of the optics;
Nd=1;                 % number of detectors;
Nsc=0.75;              % scan efficiency;
D=0.055;              % aperture (m)
% detectivity (cm-Hz^(1/2)-watt(-1) = (calculated from NET)
Deestar=4.12866e10;
taup=0.85;              % transmission of the polarizer
% derivative of Planck's Equation (relative to 262°K)
dndT=4.00e-5;

% NET calculation
NET_numerator=20*F*(FOVx*FOVy*Fr*Nos*Nss)^(0.5);
NET_denominator=taup*tau0*((pi*Nd*Nsc).^(0.5))*(D^2)*deltax
                  *deltay*Deestar*dndT;
NET=NET_numerator/NET_denominator;

% spatial frequency
f0=linspace(0,0.55,400);

% noise filter factor calculation
rb=0.335;              %
rox=(1+(2*f0*rb).^2).^(-0.5);

% fitting curve to allow better interpolation
MTFFfit=(sinc(f0/.55)).^1.17;

% MRTD (polarized case)
MRTD_pol=2*SNRT*NET*(1./MTFFfit).*((rox).^0.5).*((((f0).^2)*
deltax*deltay/L).^0.5)*(te*Fr*Nos*Nss).^(-0.5);

% plots the results
figure(1)
plot(f_1, MRTD_1, 'x', f0, MRTD_pol, '-')
legend('Measured values', 'calculated MRTD (polarized -
filter 4)', 2)
grid

```

```

axis([0 0.55 0 50])
xlabel('spatial frequency in cycles/mrad')
ylabel('MRTD - °C')
%***** Naval Postgraduate School - CA *****
%***** Thesis Research *****
% Type : Procedure
% Name : fig5_10
% Function: plots calculated vs measured MRTD values for
%           filter 5
% Date : Jul / 1999
% Version : 1.0
% Author : Edson Fernando da Costa Guimaraes, Capt. (BAF)
% Routine Information:
%   1) calculates MRTD
%   2) plots calculated MRTD vs measured MRTD
%***** *****
%***** *****
% measured data (polarized)
clear

f_1=[0.10 0.20 0.30 0.40 0.43 0.46 0.50 0.52];
MRT_1=[0.1100 0.3400 0.8400 2.4500 3.5600 6.5600 14.1700
22.3300];
MRT_1cal=[0.0259 0.1578 0.4508 1.7640 1.5273 3.4273 5.7949
9.4493];

% AGA 780 data (polarized case)
SNRT=6.5;           % use 2.5 if only 50%Pd is required ;
deltax=1.1;          % in-scan detector subtense (mRad);
deltay=1.1;          % cross-scan detector subtense in (mRad);
L=7;                 % length to width ratio of the MRTD bar;
te=0.1;               % eye integration time (s);
Fr=6.25;              % frame rate (Hz);
Nos=1;                 % overscan ratio;
Nss=1;                 % serial scan ratio;
FOVx=(7*pi/180)*1000;    % in-scan field-of-view (mRad);
FOVy=(7*pi/180)*1000;    % cross-scan field-of-view (mRad);
F=0.20;               % focal length (m);
tau0=0.6;              % transmission of the optics;
Nd=1;                 % number of detectors;
Nsc=0.75;              % scan efficiency;
D=0.055;              % aperture (m)

```

```

% detectivity (cm-Hz^(1/2)-watt(-1) = (calculated form NET)
Deestar=4.12866e10;
taup=0.85; % transmission of the polarizer
% derivative of Planck's Equation (relative to 262°K)
dndT=4.00e-5;

% NET calculation
NET_numerator=20*F*(FOVx*FOVy*Fr*Nos*Nss)^(0.5);
NET_denominator=taup*tau0*((pi*Nd*Nsc).^(0.5))*(D^2)*deltax
                *deltay*Deestar*dndT;
NET=NET_numerator/NET_denominator;

% spatial frequency
f0=linspace(0,0.55,400);

% noise filter factor calculation
rb=0.335; %
rox=(1+(2*f0*rb).^2).^(-0.5);

% fitting curve to allow better interpolation
MTFFfit=(sinc(f0/.55)).^1.17;

% MRTD (polarized case)
MRTD_pol=2*SNRT*NET*(1./MTFFfit).*((rox).^0.5).*(((f0).^2)*
deltax*deltay/L).^0.5)*(te*Fr*Nos*Nss).^-0.5;

% Plots the results
figure(1)
plot(f_1, MRT_1, 'x', f0, MRTD_pol, '-')
legend('Measured values', 'calculated MRTD (polarized -
filter 5)', 2)
grid
axis([0 0.55 0 50])
xlabel('spatial frequency in cycles/mrad')
ylabel('MRTD - °C')

%***** Naval Postgraduate School - CA *****
%***** Thesis Research *****
% Type : Procedure
% Name : dndt
% Function: plots Planck's equation and its derivative
% Date : Jul / 1999

```

```

% Version : 1.0
% Author  : Edson Fernando da Costa Guimaraes, Capt. (BAF)
% Routine Information:
%   1) calculates M (Planck's equation)
%   2) calculates N (radiance)
%   3) calculates the derivative of Planck's equation
%   4) calculates the derivative of N
%   5) Plots M, dMdT, and dNdT
%***** ****
%***** ****
clear
close all
lambda=8:0.001:12;

% inputs the temperature
T=input('Enter T:>>');

% Planck's Equation Constants
c1=3.7418e4;
c2=1.4388e4;

% Planck's Equation
M1=(c1./(lambda.^5));
M2=exp(c2./(lambda*T))-1;
M=M1./M2;
Ni=mean(M)/pi

% The derivative of Planck's Equation
dMdT=M.*c2.*exp(c2./(lambda*T))./(lambda*(T^2).*exp(c2./(la
mbda*T)));
dNdT=dMdT/pi;
dNdT=0.001*cumsum(dNdT);

% Plot the results
figure(1)
subplot(2,1,1)
plot(lambda,M)
grid on
xlabel('lambda - micrometer')
ylabel('M')
hold on
subplot(2,1,2)
plot(lambda,dMdT)
grid on

```

```

xlabel('lambda - micrometer')
ylabel('dMdT')
figure(2)
plot(lambda, dNdT)
grid
dndt=dNdT(length(dNdT))
orient tall

%*****
%***** Naval Postgraduate School - CA *****
%***** Thesis Research *****
% Type : Procedure
% Name : enne
% Function: calculates radianc for a set of temperatures
% Date : Jul / 1999
% Version : 1.0
% Author : Edson Fernando da Costa Guimaraes, Capt. (BAF)
% Routine Information:
%   1) calculates radianc
%   2) plots the result
%   * the result is presented in Appendix D
%*****
%*****



format long
clear
close all
lambda=8:0.001:12;
Ni=[];

% initializes the sset of temperatures
for T=240:320;
  c1=3.7418e4;
  c2=1.4388e4;

  % calculates Planck's Equation
  M1=(c1./(lambda.^5));
  M2=exp(c2./(lambda*T))-1;
  M=M1./M2;
  Ni=[Ni mean(M)/pi];

  % outputs string of radianc values
  fprintf(1,['%6.0f %10.8e\n'],T,mean(M)/pi);

```

```

end

% plots the results
plot(240:320,Ni)
grid
xlabel('T')
ylabel('N')
axis([240 320 2e-4 1.4e-3])

%***** Naval Postgraduate School - CA *****
%***** Thesis Research *****
% Type : Procedure
% Name : rangeimp4
% Function: estimates range improvement using polarization
% degree
% Date : Jul / 1999
% Version : 1.0
% Author : Edson Fernando da Costa Guimaraes, Capt. (BAF)
% Routine Information:
% 1) calculates the MRTD as a function of range
% 2) plots target-to-background temperature difference
% for four polarization cases (0%, 10%, 20%, and 30%);
% using table in Appendix D
%***** *****
%***** *****
format long
clear
close all
lambda=8:0.001:12;

% results presented in table 5.2 (using table D.1)
deltaT1=12.7;
deltaT2=18;
deltaT3=23.7;

% Using Searad data with the following parameters:
% • Lowtran7 was selected
% • Type of atmospheric path: Slant path between two
% altitudes
% • Surface albedo of earth: assumed blackbody
% • Navy maritime model

```

```

% • No clouds or rain
% • Altitude 1: 0
% • Altitude 2: 300ft
% • Wind speed: 7.5 m/s
% • Wind speed: 7.5 m/s (24h average)
% • Relative Humidity:
% • Airmass character: 3
% • Visibility: entered 0 (means that the program will use
%               the standard data for the chosen condition
%               <Mid-latitude summer>)

Range=linspace(0,40,400);

% Seearad Data
Title=['300ft'];
r=[0 1 2 3 4 5 10 15 20 25 30 35 40];
t=[1 0.7326 0.5784 0.4634 0.3745 0.3044 0.1155 0.0465
0.0194 0.0083 0.0036 0.0016 0];
y=[];

% linearly filling the spaces between two data points
for j=1:12
    temp=linspace(t(j),t(j+1),(r(j+1)-r(j))*10+1);
    temp(length(temp))=[];
    y=[y temp];
end

% This function calculates the MRTD
mrtd_plot
close all

R0=f0*2*15;           % 15m = critical dimension of ship

% Plotting

figure(1)
plot(Range,y*10,Range, y*deltaT1,Range, y*deltaT2,Range,
y*deltaT3,R0,MRTD_300,R0,MRTD_pol)
xlabel('Range (km)')
ylabel('TBTD')
axis([0 25 0 5])
grid

figure(2)

```

```

plot(Range,y*10,Range, y*deltaT1,Range, y*deltaT2,Range,
y*deltaT3,R0,MRTD_300,R0,MRTD_pol)
xlabel('Range (km)')
ylabel('TBTD')
axis([8 14 0.5 2.5])
grid
gtext('POL=0%')
gtext('POL=10%')
gtext('POL=20%')
gtext('POL=30%')
gtext('MRTD - with polarizer')
gtext('MRTD - without polarizer')

figure(3)
plot(R0,MRTD_300,R0,MRTD_pol,:')
axis([0 16 0 10])
xlabel('Range (km)')
ylabel('MRTD')
grid
legend('MRTD - without polarizer','MRTD - with
polarizer',0)

```

```

*****
***** Naval Postgraduate School - CA *****
***** Thesis Research *****
% Type      : Procedure
% Name      : rangeimp5
% Function: estimates range improvement using Lagaras
%           [Ref. 11] data
% Date      : Jul / 1999
% Version   : 1.0
% Author    : Edson Fernando da Costa Guimaraes, Capt. (BAF)
% Routine Information:
%   1) calculates the MRTD as a function of range
%   2) plots target-to-background temperature difference
%      for polarized and unpolarized cases
*****
***** format long
***** clear
***** close all
***** lambda=8:0.001:12;

```

```

% Using Seearad data with the following parameters:
% . Lowtran7 was selected
% . Type of atmospheric path: Slant path between two
% altitudes
% . Surface albedo of earth: assumed blackbody
% . Navy maritime model
% . No clouds or rain
% . Altitude 1: 0
% . Altitude 2: 300ft
% . Wind speed: 7.5 m/s
% . Wind speed: 7.5 m/s (24h average)
% . Relative Humidity:
% . Airmass character: 3
% . Visibility: entered 0 (means that the program will use
% the standard data for the chosen conditions
% <Mid-latitude summer>)

Range=linspace(0,40,400);

% Lagaras data
range1=[1.5 3.5 5 7 8 9 11 13 15.5 16.5 19 20 21 22 25
25.5 27 29 31 33 40];
unp=[15.7 12.8 11 9 8 7.5 6.4 5 4 3.5 3 2.6 2.5 2.4 2 1.8
1.5 1.4 1 0.7 0];
range2=[1.5 3.5 4.5 7 8 9 11 13 15.5 16.5 19 20 22 25 40];
pol=[36 29 27 21 19 17.5 14.5 12 8.9 8.15 6 5.5 4.6 3.5
0];

% interpolation process
XI=0:0.1:40;
YI1 = INTERP1(range1,unp,XI,'cubic');
YI2 = INTERP1(range2,pol,XI,'cubic');

% This function calculates the MRTD
mrtd_plot
close all

R0=f0*2*15;           % 15m = critical dimension of ship

% Plotting
figure(1)      % this is figure 5.15 in chapter V
plot(range1,unp, 'bo', range2,pol, 'rx',XI,YI1,'b',
XI,YI2,'r')

```

```

grid
xlabel('Range (km)')
ylabel('TBTD')
legend('Unpolarized','Polarized',0)

figure(2)      % this is figure 5.16 in chapter V
plot(XI,YI1,'b',XI,YI2,'r:',R0,MRTD_300,'b',R0,MRTD_pol,'r:
')
xlabel('Range (km)')
ylabel('TBTD')
axis([0 25 0 25])
grid
legend('Unpolarized','Polarized',0)

figure(3)      % this is figure 5.16 in chapter V
plot(XI,YI1,'b',XI,YI2,'r:',R0,MRTD_300,'b',R0,MRTD_pol,'r:
')
xlabel('Range (km)')
ylabel('TBTD')
axis([13 16 3 10])
grid
legend('Unpolarized','Polarized',0)

```

```

*****
%***** Naval Postgraduate School - CA *****
%***** Thesis Research *****
% Type      : Procedure
% Name      : fig6_1d
% Function: compares experimental and calculated data
% Date      : Jul / 1999
% Version   : 1.0
% Author    : Edson Fernando da Costa Guimaraes, Capt. (BAF)
% Routine Information:
%     1) plots calculated MRTD vs measured MRTD
%        (unpolarized)
%     2) plots calculated MRTD vs measured MRTD (polarized)
%*****
%*****

```

```

clear

% measured data (unpolarized)
f_0=[0.1 0.2 0.3 0.4 0.5 0.52];

```

```

MRT_0=[0.1 0.3 0.64 1.84 7.17 13.72];
MRT_0cal=[0.05 0.17 0.63 2.27 4.86 10.13];

% measured data (polarized - filter 4)
f_4=[0.10 0.20 0.30 0.40 0.43 0.46 0.50 0.52];
MRT_4=[0.5600 0.7200 1.1700 2.0600 3.6700 6.4400 13.7200
40.9500];
MRT_4cal=[0.0974 0.1793 0.7638 1.1012 1.6141 2.6747 5.7369
23.0554];

% measured data (polarized - filter 5)
f_5=[0.10 0.20 0.30 0.40 0.43 0.46 0.50 0.52];
MRT_5=[0.1100 0.3400 0.8400 2.4500 3.5600 6.5600 14.1700
22.3300];
MRT_5cal=[0.0259 0.1578 0.4508 1.7640 1.5273 3.4273 5.7949
9.4493];

% AGA 780 data (polarized case)
SNRT=6.5; % use 2.5 if only 50%Pd is required ;
deltax=1.1; % in-scan detector subtense (mRad);
deltay=1.1; % cross-scan detector subtense in (mRad);
L=7; % length to width ratio of the MRTD bar;
te=0.1; % eye integration time (s);
Fr=6.25; % frame rate (Hz);
Nos=1; % overscan ratio;
Nss=1; % serial scan ratio;
FOVx=(7*pi/180)*1000; % in-scan field-of-view (mRad);
FOVy=(7*pi/180)*1000; % cross-scan field-of-view (mRad);
F=0.20; % focal length (m);
tau0=0.6; % transmission of the optics;
Nd=1; % number of detectors;
Nsc=0.75; % scan efficiency;
D=0.055; % aperture (m)

% detectivity (cm-Hz^(1/2)-watt(-1) = (calculated from NET)
Deestar=4.12866e10;
taup=0.85; % transmission of the polarizer

% derivative of Planck's Equation (relative to 262°K)
dndT=4.00e-5;

% NET calculation
NET_numerator=20*F*(FOVx*FOVy*Fr*Nos*Nss)^(0.5);
NET_denominator=taup*tau0*((pi*Nd*Nsc).^(0.5))*(D^2)*deltax
*deltay*Deestar*dndT;

```

```

NET=NET_numerator/NET_denominator;

% spatial frequency
f0=linspace(0,0.55,400);

% noise filter factor calculation
rb=0.335; %
rox=(1+(2*f0*rb).^2).^(-0.5);

% fitting curve to allow better interpolation
MTFFfit=(sinc(f0/.55)).^1.17;

% MRTD (polarized case)
MRTD_pol=2*SNRT*NET*(1./MTFFfit).*((rox).^0.5).*(((f0).^2)*
deltax*deltay/L).^0.5)*(te*Fr*Nos*Nss).^-0.5;

% AGA 780 data (unpolarized case)
dndT=6.27e-5; % derivative of Planck's Equation
(relative to 300°K)

% NET calculation
NET_numerator=20*F*(FOVx*FOVY*Fr*Nos*Nss)^0.5;
NET_denominator=tau0*((pi*Nd*Nsc).^(0.5))*(D^2)*deltax*delt
ay*Deestar*dndT;
NET=NET_numerator/NET_denominator;

% MRTD (unpolarized case)
MRTD_300=2*SNRT*NET*(1./MTFFfit).*((rox).^0.5).*(((f0).^2)*
deltax*deltay/L).^0.5)*(te*Fr*Nos*Nss).^-0.5;

% plots the results
figure(2)
plot(f_0, MRT_0, 'bx', f_4, MRT_4, 'ro', f_5, MRT_5, 'rs',
f0,MRTD_300,'b-', f0,MRTD_pol,'r:')
legend('Measured unpolarized', 'Measured vertical pol.
', 'Measured horizontal pol.', 'calculated MRTD unpol.',
'calculated MRTD pol.',2)
grid
axis([0 0.55 0 20])
xlabel('spatial frequency in cycles/mrad')
ylabel('MRTD - °C')

```

```

%***** Naval Postgraduate School - CA *****
%***** Thesis Research *****
% Type : Procedure
% Name : readptw2
% Function: reads *.ptw files generated by PTRwin
% Date : May / 1999
% Version : 1.0
% Author : Edson Fernando da Costa Guimaraes, Capt. (BAF)
% Routine Information:
%   1) It reads a *.ptw file and plots it as a figure and
%      also plots a 3D view of the image.
%   2) It allows the user to select a detail to be
%      analyzed.
%   3) It plots the profile of the detail.
%   4) It allows the user to select the peaks and valleys
%      of the profile.
%   5) It performs a fourier analysis of the profile.
%   6) It generates a string output to the file
%      "summary.dat" with the basic information of the
%      file: name, spatial frequency, target temperature,
%      background temperature, thermal range, thermal
%      level, peak temperature, valley temperature, type of
%      filter used.
%*****
```

```

% creates output file 'summary.dat'
fid0=fopen('summary.dat','wr');
f=1;
while f~=0
%open the *.ptw file
f=uigetfile('*.*ptw');
fid=fopen(f,'r');
pol=input('Enter the filter used (0, 4, 5):');

% locate the thermal level in the file
gap1=65536;
status=fseek(fid,gap1,'bof');
level=fread(fid,1,'int16');

% locate the thermal range in the file
gap2=65536+40;
status=fseek(fid,gap2,'bof');
range=fread(fid,1,'int16');
```

```

% locate the image in the file
gap=65536+3072;
status=fseek(fid,gap,'bof');
A=fread(fid,[16000,4],'int16');
field1=reshape(A(:,1),250,64);
field2=reshape(A(:,2),250,64);
field3=reshape(A(:,3),250,64);
field4=reshape(A(:,4),250,64);
picture=[];

% build the image with the fields
for n=1:64

    temp=[field1(:,n)';field2(:,n)';field3(:,n)';field4(:,n)'];
    picture=[picture,temp];
end
close all

% plot the image as a surface
figure(1)
surf(picture)
view(0,90)

% select a detail
title('click on the upper left corner of the detail')
[d1,d2]=ginput(1);
title('click on the lower right corner of the detail')
[d3,d4]=ginput(1);
title('')

% plot the detail
figure(2)
detail=picture(round(d4):round(d2),round(d1):round(d3));
%%%integers
surf1(detail)
shading interp;
colormap(pink)
title(['3D view of the output - file: ',f])

% calculate and plot the profile
figure(3)
[x,y]=size(detail);
profile=detail(round(x/2),:); %%integers

```

```

% transform digital level in temperature
for z=1:length(profile)
    profile(z)=dl2temp(profile(z),level,range,pol);
end
plot(profile)
grid

% select peaks and valleys
title('select the four apparent peaks, using the mouse')
[px,py]=ginput(4);
title('select the three apparent valleys, using the mouse')
[vx,vy]=ginput(3);
peak=mean(py);
valley=mean(vy);
text(mean(px),peak,['mean peak is: ',num2str(peak), '°C']);
text(mean(px),valley,['mean valley is:
',num2str(valley), '°C']);

title(['Horizontal profile of the output - file: ',f])
orient tall

% allow user to enter file parameters
clc
spatial_freq=input('Enter the spatial frequency used in
this file:');
Tb=input('Enter the recorded background temperature
(Tb):');
Tt=input('Enter the recorded target temperature (Tt):');
MRTD=Tb-Tt;
MRTDcal=0.1*MRTD/(peak-valley);
fprintf(fid0,[f, '%6.2f %6.2f %6.2f %6.2f %6.2f %8.4f %8.4f
%8.4f %8.4f %1i\n'],...
spatial_freq,Tt,Tb,level,range,peak,valley,MRTD,MRTDcal,pol
);
end
fclose('all');

```

```

***** Naval Postgraduate School - CA ****
***** Thesis Research ****
% Type : Procedure
% Name : readmtf
% Function: reads MTF information from selected *.ptw files
% generated by PTRwin.
% Date : May / 1999
% Version : 1.0
% Author : Edson Fernando da Costa Guimaraes, Capt. (BAF)
% Routine Information:
% 1) It reads a *.ptw file and plots it as a figure and
% also plots a 3D view of the image.
% 2) It allows the user to select a detail to be
% analyzed.
% 3) It plots the profile of the detail.
% 4) It allows the user to select the peaks and valleys
% of the profile.
% 5) It generates a string output with the basic
% information of the file: name, peak temperature, and
% valley temperature.
*****
```

```

f=1;
while f~=0
    % open the *.ptw file
    clear
    f=uigetfile('mtf*.ptw');
    fid=fopen(f,'r');

    % locate the thermal level in the file
    gap1=65536;
    status=fseek(fid,gap1,'bof');
    level=fread(fid,1,'int16');

    % locate the thermal range in the file
    gap2=65536+40;
    status=fseek(fid,gap2,'bof');
    range=fread(fid,1,'int16');

    % locate the image in the file
    gap=65536+3072;
    status=fseek(fid,gap,'bof');
    A=fread(fid,[16000,4],'int16');
```

```

field1=reshape(A(:,1),250,64);
field2=reshape(A(:,2),250,64);
field3=reshape(A(:,3),250,64);
field4=reshape(A(:,4),250,64);
picture=[];

% build the image with the fields
for n=1:64

temp=[field1(:,n)';field2(:,n)';field3(:,n)';field4(:,n)'];
picture=[picture,temp];
end
close all

% plot the image
figure(1)
imagesc(picture);
title (['Image: ',f]);

% plot the image as a surface
figure(2)
surf(picture)
view(0,90)

% select a detail
title('click on the upper left corner of the detail')
[d1,d2]=ginput(1);
title('click on the lower right corner of the detail')
[d3,d4]=ginput(1);
title('')

detail=picture(round(d4):round(d2),round(d1):round(d3));
%%%integers

% calculate and plot the profile
figure(4)
[x,y]=size(detail);
profile=detail(round(x/2),:); %%%integers

% select peaks and valleys
plot(profile)
grid
title('select the four apparent peaks, using the mouse')
[px,py]=ginput(4);

```

```

    title('select the three apparent valleys, using the
mouse')
    [vx,vy]=ginput(3);
    peak=mean(py);
    valley=mean(vy);
    text(mean(px),peak,['mean peak is: ',num2str(peak),'
DL']);
    text(mean(px),valley,['mean valley is:
',num2str(valley),',DL']);
    title(['Horizontal profile of the output - file: ',f])
    orient tall

    % outputs string of information
    fprintf(1,[f,'%8.4f %8.4f\n'],peak,valley);

end

```

```

%***** Naval Postgraduate School - CA *****
%***** Thesis Research *****
% Type : Procedure
% Name : filt
% Function: set filter to program readgui
% Date : Jul / 1999
% Version : 1.0
% Author : Edson Fernando da Costa Guimaraes, Capt. (BAF)
%***** *****
%***** *****

```

```

function fig = filt()
% This is the machine-generated representation of a Handle
% Graphics object and its children. Note that handle values
% may change when these objects are re-created. This may
% cause problems with any callbacks written to depend on
% the value of the handle at the time the object was saved.
% To reopen this object, just type the name of the M-file
% at the MATLAB prompt. The M-file and its associated MAT
% -file must be on your path.

```

```

load filt

h0 = figure('Color',[0.8 0.8 0.8], ...
'Colormap',mat0, ...

```

```

'PointerShapeCData',mat1, ...
'Position',[601 361 363 85], ...
'Tag','Fig1');
h1 = uicontrol('Parent',h0, ...
'Units','points', ...
'Callback','warning off,global p,p=0;warning on,close',
...
'ListboxTop',0, ...
'Position',[23.58620689655173 6.827586206896553
47.17241379310346 17.37931034482759], ...
'String','0', ...
'Tag','Pushbutton1');
h1 = uicontrol('Parent',h0, ...
'Units','points', ...
'Callback','warning off,global p,p=5;warning on,close',
...
'ListboxTop',0, ...
'Position',[162 6.827586206896553 47.17241379310346
17.37931034482759], ...
'String','5', ...
'Tag','Pushbutton1');
h1 = uicontrol('Parent',h0, ...
'Units','points', ...
'Callback','warning off,global p,p=4;warning on,close',
...
'ListboxTop',0, ...
'Position',[94.34482758620692 6.206896551724139
47.17241379310346 17.37931034482759], ...
'String','4', ...
'Tag','Pushbutton1');
h1 = uicontrol('Parent',h0, ...
'Units','points', ...
'BackgroundColor',[0.752941176470588 0.752941176470588
0.752941176470588], ...
'ListboxTop',0, ...
'Position',[44.6896551724138 29.79310344827587
141.5172413793104 15.51724137931035], ...
'String','Select Filter', ...
'Style','text', ...
'Tag','StaticText1');
if nargout > 0, fig = h0; end

```

```

%***** Naval Postgraduate School - CA ***** Thesis Research *****
% Type : Function
% Name : gu1
% Function: support the Graphical User Interface (GUI) for
%           program readgui.
% Date : Jul / 1999
% Version : 1.0
% Author : Edson Fernando da Costa Guimaraes, Capt. (BAF)
% Routine Information:
%   1) loads figure from file
%   2) gets a detail
%   3) calculates the profile
%   4) allows selection of peaks and valleys
%   5) allows frequency domain analysis
%   6) plots detail in 3D
%*****
%*****

```

```

function gu1(action)
global p; % polarization
colormap('default')
global fid picture f detail profile level range vy peak
valley
switch action
case 'load' % loads figure from file
  f=uigetfile('*.*ptw'); % opens file
  fid=fopen(f,'r');
  gap1=65536; % skips the header
  status=fseek(fid,gap1,'bof');
  level=fread(fid,1,'int16'); % reads thermal level
  gap2=65536+40;
  status=fseek(fid,gap2,'bof');
  range=fread(fid,1,'int16'); % reads thermal range

  gap=65536+3072;
  status=fseek(fid,gap,'bof');
  A=fread(fid,[16000,4],'int16'); % reads frame
  field1=reshape(A(:,1),250,64); % extracts field #1
  field2=reshape(A(:,2),250,64); % extracts field #2
  field3=reshape(A(:,3),250,64); % extracts field #3
  field4=reshape(A(:,4),250,64); % extracts field #4
  picture=[];

```

```

%builds the picture from fields
for n=1:64

    temp=[field1(:,n)';field2(:,n)';field3(:,n)';field4(:,n)']
];
    picture=[picture,temp];
end

% plots image
imagesc(picture);
title (['Image: ',f]);

case 'detail' % gets a detail
imagesc(picture);
title (['Image: ',f]);

% allows selection of detail limits
title('click on the upper left corner of the detail')
[x1,x2]=ginput(1);
title('click on the lower right corner of the detail')
[x3,x4]=ginput(1);
title('')

% plots detail
detail=picture(min(round(x4),round(x2)):max(round(x4),round(x2)),min(round(x1),round(x3)):max(round(x1),round(x3)));
%%integers
surf(detail)
[a,b]=size(detail);
axis([1 b 1 a 0 max(max(detail))])
view(0,90)
title (['Detail: ',f]);
% asks for polarization number through function "filt"
filt;
but3=findobj(gcbf,'Tag','profile');
set(but3,'Enable','on');

case 'profile' % calculates the profile

[x,y]=size(detail);
profile=detail(round(x/2),:) %%integers
% transforms digital level in isothermal units
% profile=profile*range/4095+level-range/2;
% transforms digital level in isothermal units

```

```

for z=1:length(profile)
profile(z)=d12temp(profile(z),level,range,p);
end

plot(profile)
grid

% enables button "peak"
but1=findobj(gcbf,'Tag','peak');
set(but1,'Enable','on');
but3=findobj(gcbf,'Tag','profile');
set(but3,'Enable','off');

case 'peak' %allows selection of peaks and valleys
title('select the four apparent peaks, using the mouse')
[px,py]=ginput(4);
title('select the three apparent valleys, using the
mouse')
[vx,vy]=ginput(3);
peak=mean(py);
valley=mean(vy);
text(mean(px),peak,['mean peak is:
',num2str(peak),'^\circ C']);
text(mean(px),valley,['mean valley is:
',num2str(valley),'^\circ C']);
title(['Horizontal profile of the output - file: ',f])
but1=findobj(gcbf,'Tag','peak');
set(but1,'Enable','off');

% enables button "fourier"
but2=findobj(gcbf,'Tag','fourier');
set(but2,'Enable','on');

case 'three' % plots detail in 3D
surf(detail)
shading interp;
colormap(pink)
title(['3D view of the output - file: ',f])

case 'fourier' % allows frequency domain analysis
minv=min(vy);
shadow=find(profile/minv>=1);
mask=zeros(1,length(profile));
mask(shadow)=1;

```

```

profile1=profile.*mask;
mask(shadow)=(peak+valley)/2;
profile2=profile1-mask;

NET=0.12;
y=abs(log10(length(profile2))/log10(2));
F=fft(profile2)/(2^y);
F=fftshift(F);
mu=(-length(profile2)/2:length(profile2)/2-
1)^1/length(profile2);

plot(mu,abs(F))
hold on
plot(mu,min(abs(F))*6*ones(length(profile2)),'r')
hold off
axis([min(mu) max(mu) 0 max(max(abs(F)),min(abs(F))*6)])
but2=findobj(gcbf,'Tag','fourier');
set(but2,'Enable','off');

end

%*****
%***** Naval Postgraduate School - CA *****
%***** Thesis Research *****
% Type      : Function
% Name      : readgui
% Function: Graphical User Interface (GUI) equivalent to
%           function readptw2.m that reads *.ptw files
%           generated by PTRwin
% Date      : Jul / 1999
% Version   : 1.0
% Author    : Edson Fernando da Costa Guimaraes, Capt. (BAF)
% Routine Information:
%   1) loads figure from file
%   2) gets a detail
%   3) calculates the profile
%   4) allows selection of peaks and valleys
%   5) allows frequency domain analysis
%   6) plots detail in 3D
%*****
%***** function fig = readgui()

```

```
% This is the machine-generated representation of a Handle
% Graphics object and its children. Note that handle values
% may change when these objects are re-created. This may
% cause problems with any callbacks written to depend on
% the value of the handle at the time the object was saved.
% To reopen this object, just type the name of the M-file
% at the MATLAB prompt. The M-file and its associated MAT
% -file must be on your path.
```

```
load readgui

h0 = figure('Units','points', ...
'Color',[0.8 0.8 0.8], ...
'Colormap',mat0, ...
'PointerShapeCData',mat1, ...
'Position',mat2, ...
' Renderer','zbuffer', ...
' RendererMode','manual', ...
' Tag','Fig1');
h1 = uicontrol('Parent',h0, ...
'Units','points', ...
'BackgroundColor',[0.752941176470588 0.752941176470588
0.752941176470588], ...
'FontSize',28, ...
'ForegroundColor',[0.3 0.3 0.3], ...
'ListboxTop',0, ...
'Position',[60.82758620689656 261.9310344827587
325.8620689655173 32.89655172413794], ...
'String','Welcome to Readptw.m', ...
'Style','text', ...
'Tag','StaticText1');
h1 = uicontrol('Parent',h0, ...
'Units','points', ...
'Callback','gui1(''load'')', ...
'ListboxTop',0, ...
'Position',[290.4827586206897 205.448275862069
72.62068965517243 29.17241379310346], ...
'String','Load PTW', ...
'Tag','PushButton1');
h1 = uicontrol('Parent',h0, ...
'Units','points', ...
'Callback','gui1(''three'')', ...
'ListboxTop',0, ...
'Position',[290.4827586206897 64.55172413793105
72.62068965517243 29.17241379310346], ...
```

```

'String','3D View', ...
'Tag','Pushbutton1');
h1 = uicontrol('Parent',h0, ...
'Units','points', ...
'Callback','guil(''profile'')', ...
'Enable','off', ...
'ListboxTop',0, ...
'Position',mat3, ...
'String','Profile', ...
'Tag','profile');
h1 = uicontrol('Parent',h0, ...
'Units','points', ...
'Callback','fclose(''all'');close(gcbf)', ...
'ListboxTop',0, ...
'Position',[290.4827586206897 19.24137931034483
72.62068965517243 29.17241379310346], ...
'String','Exit', ...
'Tag','Pushbutton1');
h1 = uicontrol('Parent',h0, ...
'Units','points', ...
'Callback','guil(''detail'')', ...
'ListboxTop',0, ...
'Position',[290.4827586206897 160.1379310344828
72.62068965517243 29.17241379310346], ...
'String','Detail', ...
'Tag','Pushbutton1');
h1 = uicontrol('Parent',h0, ...
'Units','points', ...
'Callback','guil(''peak'')', ...
'Enable','off', ...
'ListboxTop',0, ...
'Position',[39.10344827586208 16.44827586206897
93.10344827586209 16.75862068965517], ...
'String','Peak & Valley', ...
'Tag','peak');
h1 = uicontrol('Parent',h0, ...
'Units','points', ...
'Callback','guil(''fourier'')', ...
'Enable','off', ...
'ListboxTop',0, ...
'Position',[157.0344827586207 16.44827586206897
93.10344827586209 16.75862068965517], ...
'String','Fourier Transform', ...
'Tag','fourier');
h1 = axes('Parent',h0, ...

```

```

'Units','pixels', ...
'Box','on', ...
'CameraUpVector',[0 1 0], ...
'CameraUpVectorMode','manual', ...
'Color',[1 1 1], ...
'ColorOrder',mat4, ...
'Position',[66 106 337 271], ...
'Tag','Axes1', ...
'XColor',[0 0 0], ...
'YColor',[0 0 0], ...
'ZColor',[0 0 0]);
h2 = line('Parent',h1, ...
'Color',[0 0 1], ...
'Tag','Axes1Line1', ...
'XData',0, ...
'YData',0);
h2 = text('Parent',h1, ...
'Color',[0 0 0], ...
'HandleVisibility','off', ...
'HorizontalAlignment','center', ...
'Position',[-0.005952380952380931 -1.207407407407407
17.32050807568877], ...
'Tag','Axes1Text4', ...
'VerticalAlignment','cap');
set(get(h2,'Parent'),'XLabel',h2);
h2 = text('Parent',h1, ...
'Color',[0 0 0], ...
'HandleVisibility','off', ...
'HorizontalAlignment','center', ...
'Position',[-1.238095238095238 -0.007407407407407085
17.32050807568877], ...
'Rotation',90, ...
'Tag','Axes1Text3', ...
'VerticalAlignment','baseline');
set(get(h2,'Parent'),'YLabel',h2);
h2 = text('Parent',h1, ...
'Color',[0 0 0], ...
'HandleVisibility','off', ...
'HorizontalAlignment','right', ...
'Position',[-1.392857142857143 1.940740740740741
17.32050807568877], ...
'Tag','Axes1Text2', ...
'Visible','off');
set(get(h2,'Parent'),'ZLabel',h2);
h2 = text('Parent',h1, ...

```

```
'Color',[0 0 0], ...
'HandleVisibility','off', ...
'HorizontalAlignment','center', ...
'Position',mat5, ...
'Tag','Axes1Text1', ...
'VerticalAlignment','bottom');
set(get(h2,'Parent'),'Title',h2);
if nargout > 0, fig = h0; end
```

APPENDIX B. LABORATORY SETUP

In order to measure the Minimum Resolvable Temperature Difference, the electro-optics laboratory was prepared to be used with the setup shown in Figure B.1 and described in this Appendix.

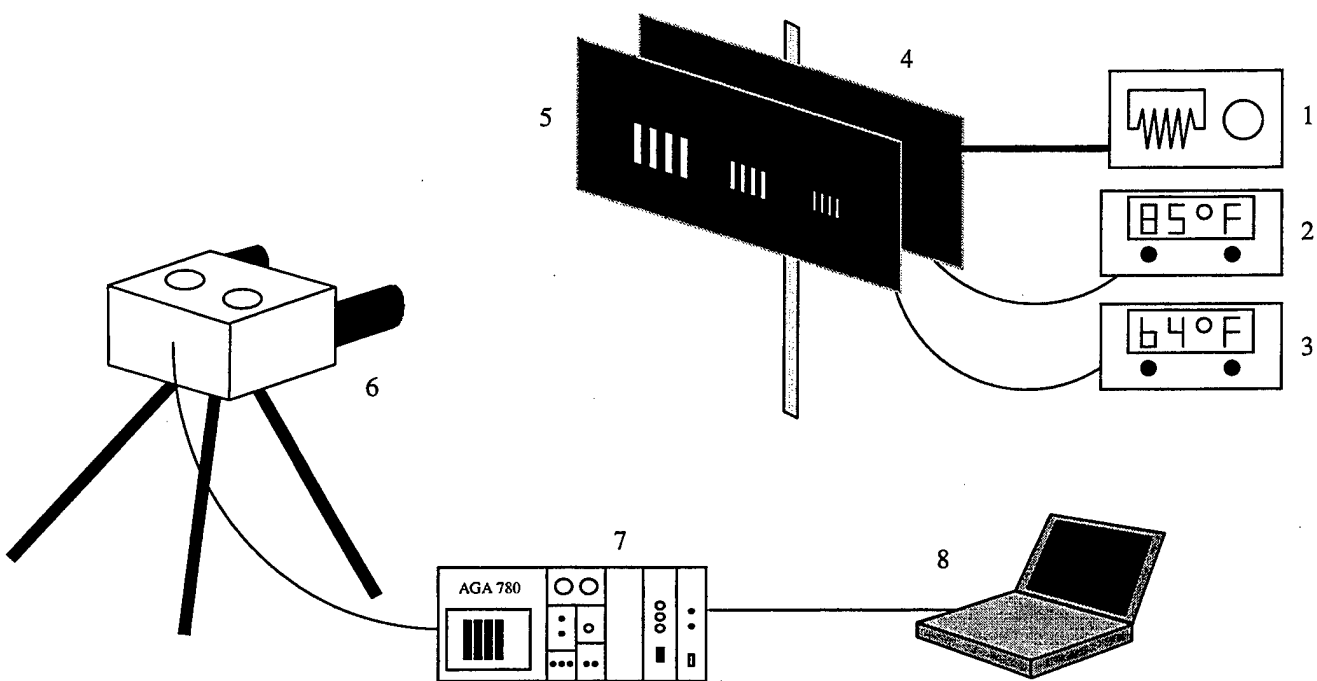


Figure B.1 - Laboratory Setup for Measurement of MRTD.

1. Autotransformer Variac® type WIOMT3 (General Radio Company), with output voltage variable from 0 to 140V (10 Amps). This equipment was used to heat the background plate by varying the voltage applied to

a resistance installed on the backside of the plate (4).

2. Digital Thermometer model 2190A (Fluke). This equipment displays either Centigrade or Fahrenheit values, both with a precision of 1 unit. All the measurements were taken in degrees Fahrenheit in order to improve the precision ($1^{\circ}\text{F} \sim 0.555^{\circ}\text{C}$). This thermometer was used to display the temperature of the back plate (4) corresponding to the background. The equipment precision is not satisfactory for MRTD measurements. Equipment precision should be improved if further measurements are to be taken.

3. Same as <2>, but used to display the temperature of the front plate (5).

4. Back plate. This plate represents the background with a emissivity of 0.9.

5. Front plate. This plate represents the target (kept at room temperature) and contains the standard MRTD pattern (7:1 aspect ratio) as shown in Figure B.2.

6. AGA Thermovision 780. It is a two channel infrared scanning system with single detector. It operates in both MWIR ($3\text{-}5\mu\text{m}$) and LWIR ($8\text{-}12\mu\text{m}$) [Ref. 4]. For

this thesis, only the LWIR band, with the HgCdTe detector, was used.

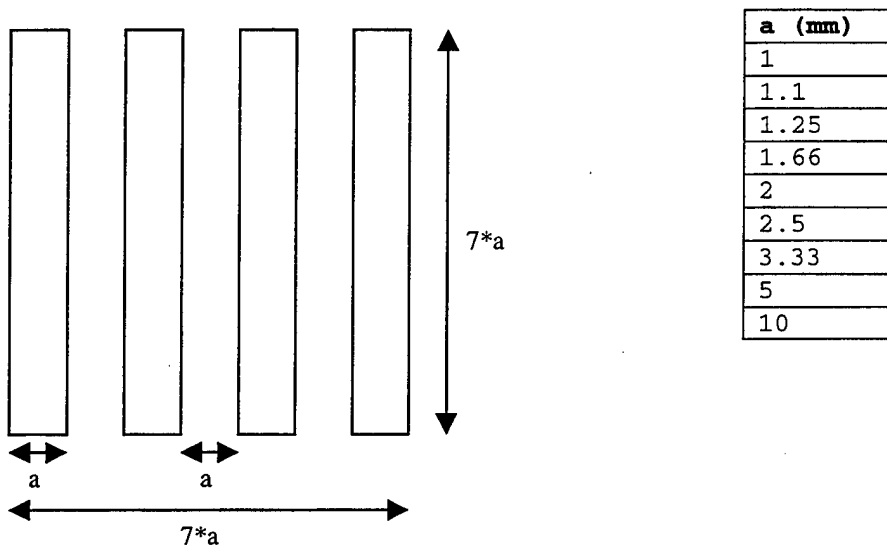


Figure B.2 - MRTD Pattern.

7. Black and white monitor chassis. It was used as an interface between the camera (6) and the computer. Although it is the original display of the AGA 780, most of its functions were performed by the NEC computer (8), which provides an extended set of resources for recording and analyzing the images.
8. NEC laptop computer VERSA P75 (Pentium® 75 MHz) installed with PTRWIN® v3.16 software. This software was used for acquisition and analysis of the images received from the AGA 780. Using a 12-bit A/D converter, it converts detector signal

intensity into 4096 discrete digital levels. [Ref.

12]

APPENDIX C. SUMMARY OF THE IMAGES

Tables C.1 to C.3 show a summary of the most important data extracted from the images collected in this experiment. The fields in this table are: file name (File), spatial frequency (Freq), background temperature (Tb - converted to °C), target temperature (Tt), thermal level (TL), thermal range (TR), temperature of the peak (Tp), temperature of the valley (Tv), MRTD, calibrated MRTD (MRTDcal), polarizer (p), and date of collection (Date).

File	Freq	Tb	Tt	TL	TR	Tp	Tv	MRTD	MRTDcal	p	Date
A_lun00.ptw	0.43	20.4	20	52	2	22.16	22.23	-0.40	0.54	0	10/may
A_lun01.ptw	0.45	20.2	21.7	52	2	22.69	22.63	1.50	2.37	0	10/may
A_lun02.ptw	0.47	20.2	22.3	52	2	23.08	23.03	2.10	4.28	0	10/may
A_lun03.ptw	0.5	20.2	25.3	54	2	25.79	25.69	5.10	5.01	0	10/may
A_lun04.ptw	0.52	21	32.6	56	5	29.41	29.25	11.60	7.06	0	10/may
A_f00.ptw	0.1	24.3	24.2	51	2	20.15	20.35	-0.10	0.05	0	25/may
A_f02.ptw	0.2	24.3	24.6	85	2	61.04	60.87	0.30	0.17	0	25/may
A_f03.ptw	0.3	24.3	24.94	51	2	20.87	20.76	0.64	0.63	0	25/may
A_f04.ptw	0.4	24.33	26.17	51	2	20.97	20.89	1.84	2.27	0	25/may
A_f05.ptw	0.5	24.44	31.61	52	5	23.55	23.40	7.17	4.86	0	25/may
A_f07.ptw	0.52	24.61	38.33	56	5	27.81	27.68	13.72	10.13	0	25/may
A_unp00.ptw	0.3	22.3	24.2	54	2	26.26	25.89	1.90	0.51	0	06/may
A_unp01.ptw	0.4	22.2	24.2	54	2	26.34	26.22	2.00	1.65	0	06/may
A_unp04.ptw	0.48	23.5	41	59	20	35.44	35.00	17.50	3.91	0	06/may
A_unp06.ptw	0.43	23.2	33.7	61	5	32.46	32.13	10.50	3.20	0	06/may
A2_un01.ptw	0.1	23.39	23.33	55	2	25.66	25.78	-0.06	0.05	0	11/may
A2_un02.ptw	0.2	23.33	23.61	54	2	24.86	24.70	0.28	0.17	0	11/may
A2_un03.ptw	0.3	23.33	24	54	2	25.05	24.95	0.67	0.62	0	11/may
A2_un04.ptw	0.4	23.5	24.78	55	2	26.06	25.95	1.28	1.17	0	11/may
A2_un05.ptw	0.5	23.72	40.28	62	10	34.23	34.05	16.56	9.07	0	11/may

Table C.1 - Summary of Data for the Unpolarized Case.

File	Freq	Tb	Tt	TL	TR	Tp	Tv	MRTD	MRDTcal	p	Date
A_fp00.ptw	0.1	23.61	24.17	49	2	21.35	20.77	0.56	0.10	4	26/may
A_fp01.ptw	0.2	23.61	24.33	49	2	21.65	21.25	0.72	0.18	4	26/may
A_fp02.ptw	0.3	23.61	24.78	50	2	25.63	25.48	1.17	0.76	4	26/may
A_fp03.ptw	0.4	23.72	25.78	51	2	26.12	25.94	2.06	1.10	4	26/may
A_fp04.ptw	0.43	23.72	27.39	51	2	28.17	27.94	3.67	1.61	4	26/may
A_fp05.ptw	0.46	23.78	30.22	52	2	30.13	29.89	6.44	2.67	4	26/may
A_fp06.ptw	0.5	23.89	37.61	53	2	33.31	33.07	13.72	5.74	4	26/may
A_fp07.ptw	0.52	24.61	65.56	58	5	49.60	49.42	40.95	23.06	4	26/may

Table C.2 - Summary of Data (Vertically Polarized Case).

File	Freq	Tb	Tt	TL	TR	Tp	Tv	MRTD	MRDTcal	p	Date
A5_fp00.ptw	0.1	16.94	17.05	46	2	9.06	8.63	0.11	0.03	5	08/jun
A5_fp01.ptw	0.2	16.94	17.28	46	2	9.34	9.12	0.34	0.16	5	08/jun
A5_fp02.ptw	0.3	16.94	17.78	47	2	13.12	12.94	0.84	0.45	5	08/jun
A5_fp03.ptw	0.4	16.94	19.39	47	2	14.51	14.37	2.45	1.76	5	08/jun
A5_fp04.ptw	0.43	16.94	20.5	48	2	17.57	17.34	3.56	1.53	5	08/jun
A5_fp05.ptw	0.46	16.94	23.5	49	2	21.08	20.89	6.56	3.43	5	08/jun
A5_fp06.ptw	0.5	17.11	31.28	49	2	22.92	22.67	14.17	5.79	5	08/jun
A5_fp07.ptw	0.52	17.11	39.44	51	2	27.27	27.03	22.33	9.45	5	08/jun

Table C.3 - Summary of Data (Horizontally Polarized Case).

Table C.4 shows the summary of the images taken for MTF (Modulation Transfer Function) estimation. The curve fitting process was carried out using the program *mtffit.m* (Appendix A).

File	Peak (DL)	Valley (DL)	Filter
Mtf00.ptw	4083.9416	0.0000	0
Mtf01.ptw	4083.9416	0.0000	0
Mtf02.ptw	3306.5693	9.7324	0
Mtf03.ptw	2380.1703	431.4680	0
Mtf04.ptw	2753.6496	1346.7153	0
Mtf05.ptw	4083.9416	4091.2409	0
Mtf06.ptw	4083.9416	4083.9416	0

Table C.4 - MTF Data Summary.

APPENDIX D. MEAN RADIANCE (8-12 μ m)

T	$\langle N \rangle$	T	$\langle N \rangle$
240	2.86112437e-004	280	6.78699088e-004
241	2.93331304e-004	281	6.91431324e-004
242	3.00673261e-004	282	7.04314046e-004
243	3.08139196e-004	283	7.17347725e-004
244	3.15729983e-004	284	7.30532826e-004
245	3.23446490e-004	285	7.43869799e-004
246	3.31289573e-004	286	7.57359088e-004
247	3.39260078e-004	287	7.71001125e-004
248	3.47358840e-004	288	7.84796332e-004
249	3.55586687e-004	289	7.98745122e-004
250	3.63944432e-004	290	8.12847900e-004
251	3.72432883e-004	291	8.27105058e-004
252	3.81052833e-004	292	8.41516980e-004
253	3.89805068e-004	293	8.56084041e-004
254	3.98690361e-004	294	8.70806605e-004
255	4.07709477e-004	295	8.85685028e-004
256	4.16863169e-004	296	9.00719655e-004
257	4.26152180e-004	297	9.15910825e-004
258	4.35577243e-004	298	9.31258863e-004
259	4.45139079e-004	299	9.46764089e-004
260	4.54838400e-004	300	9.62426811e-004
261	4.64675906e-004	301	9.78247330e-004
262	4.74652289e-004	302	9.94225936e-004
263	4.84768227e-004	303	1.01036291e-003
264	4.95024391e-004	304	1.02665853e-003
265	5.05421439e-004	305	1.04311306e-003
266	5.15960020e-004	306	1.05972675e-003
267	5.26640770e-004	307	1.07649985e-003
268	5.37464317e-004	308	1.09343260e-003
269	5.48431278e-004	309	1.11052522e-003
270	5.59542259e-004	310	1.12777795e-003
271	5.70797856e-004	311	1.14519099e-003
272	5.82198655e-004	312	1.16276456e-003
273	5.93745229e-004	313	1.18049883e-003
274	6.05438143e-004	314	1.19839401e-003
275	6.17277952e-004	315	1.21645027e-003
276	6.29265200e-004	316	1.23466779e-003
277	6.41400419e-004	317	1.25304673e-003
278	6.53684133e-004	318	1.27158725e-003
279	6.66116855e-004	319	1.29028950e-003
		320	1.30915361e-003

Table D.1 - Mean Radiance.

LIST OF REFERENCES

1. Cooper, A. W., Lentz W. J. and Walker, P. L., *Infrared Polarization Ship Images and Contrast in the MAPTIP Experiment*, SPIE Proceedings Vol.2828, 1994.
2. Holst, Gerald C., *Electro-Optical Imaging System Performance*, JCD Publishing, FL, 1995.
3. Willian L. Wolfe and George J. Zissis, *The Infrared Handbook*, Office of Naval Research, Department of the Navy, Washington, DC, 1978.
4. AGA Infrared Systems AB, *AGA Thermovision® 780 Operating Manual*, 1980
5. Kaplan, Herbert, *Practical Applications of Infrared Thermal Sensing and Imaging Equipment*, SPIE, DC, 1999
6. Khalil Seyrafi and S. A. Hovanessian, *Introduction to Electro-Optical Imaging and Tracking Systems*. Artech House, Inc. MA, 1993.
7. Shen, Liang Chi and Kong, Jin Au, *Applied Electromagnetism*, PWS Publishers, Boston, MA, 1987.
8. Shumaker, David L., J. T. Wood and C. R. Thacker, *Infrared Imaging Systems Analysis*, The Environmental Research Institute of Michigan, 1993.

9. Lloyd, Michael J., *Thermal Imaging Systems*, Plenum Press, NY, 1975.
10. Johnson, J, *Analysis of Image Forming System*, Proceedings of Image Intensifier Symposium, 1958
11. Spyridon E. Lagaras, *Modeled Detection and Recognition Range for a Polarization Filtered Sensor*, MS Thesis, Naval Postgraduate School, June, 1999.
12. Marcos C. Pontes, *Polarization Effects on Infrared Target Contrast*, MS Thesis, Naval Postgraduate School, September, 1998.
13. David G. Moretz, *Analysis of Target Contrast Improvement Using Polarization Filtering in The Infrared Region*, MS Thesis, Naval Postgraduate School, December, 1994.
14. Chih-Li Yu, *Estimate of Maximum Detection Range For FLIR From EOMET95 Measurement Data*, MS Thesis, Naval Postgraduate School, December, 1997.
15. Cooper, A. W. and E.C Crittenden, Jr, *Electro-Optic Sensors and Systems*, Naval Postgraduate School, Monterey, CA, 1995.
16. Kruse, P.W., McGlauchlin, L.D., and McQuistan, R.B., *Elements of Infrared Technology: Generation*,

Transmission, and Detection, John Willey & Sons, New York, NY, 1962.

17. *CEDIP, PTRWin Operating Manual*, Paris, France, 1980

INITIAL DISTRIBUTION LIST

1. Defense Technical Information Center 2
87725 John J. Kingman Rd., STE 0944
Ft. Belvoir, VA 22060-6218
2. Dudley Knox Library 2
Naval Postgraduate School
411 Dyer Rd.
Monterey, CA 93943-5101
3. Professor Alfred W. Cooper 2
Code PH/Cr
Naval Postgraduate School
Monterey, CA 93943-5101
4. Professor Ronald Pieper 1
Code EC/Pr
Naval Postgraduate School
Monterey, CA 93943-5101
5. Naval Sea Systems Command 1
PEO- Expeditionary Warfare
ATTN: Mr J.E. Misanin
2531 Jefferson Davis Highway
Arlington, VA 22242-5170
6. Naval Space and Naval Warfare Systems Center . 1
Propagation Division
ATTN: Dr. J.H. Richter, Code D88
53570 Silvergate Ave.
San Diego, CA 92152-5230
7. Naval Space and Naval Warfare Systems Center . 1
RDT&E Division
ATTN: Dr. D.R. Jensen, Code 833
53570 Silvergate Ave.
San Diego, CA 92152-5230

8. Naval Air Warfare Center 1
Research and Technology Group, Physics Branch
ATTN: Dr. J. Bevan
China Lake, CA 93555-6100

9. General Air Command (COMGAR) 1
Electronic Warfare Center (CGEGAR)
ATTN: Capt. Edson Guimaraes
Esplanada dos Ministerios Bloco M
Anexo - 2nd Andar
Brasilia, DF - Brazil 70045-900

10. Academia da Força Aérea 1
Biblioteca da AFA
Estrada de Aguáí, s/nº
Pirassununga, SP - Brazil 13630-000

11. Comando Aéreo de Treinamento 1
GITE
Estrada do Aeroporto, s/nº
Parnamirim, RN - Brazil 59150-000

12. Instituto Tecnológico da Aeronáutica 1
Biblioteca do ITA
Praça Mal. Eduardo Gomes, 50
São José dos Campos, SP - Brazil 12228-901

13. Professor Dan Boger 1
Chairman, Code IW
Naval Postgraduate School
Monterey, CA 93943-5101